

AWARD NUMBER: W81XWH-14-1-0271

TITLE: Targeting GPR30 in Abiraterone- and MDV3100-Resistant Prostate Cancer

PRINCIPAL INVESTIGATOR: Hung-Ming Lam, PhD

CONTRACTING ORGANIZATION: University of Washington  
Seattle WA98195

REPORT DATE: October 2016

TYPE OF REPORT: Annual

PREPARED FOR: U.S. Army Medical Research and Materiel Command  
Fort Detrick, Maryland 21702-5012

DISTRIBUTION STATEMENT: Approved for Public Release; Distribution Unlimited

The views, opinions and/or findings contained in this report are those of the author(s) and should not be construed as an official Department of the Army position, policy or decision unless so designated by other documentation.

**REPORT DOCUMENTATION PAGE***Form Approved*  
*OMB No. 0704-0188*

Public reporting burden for this collection of information is estimated to average 1 hour per response, including the time for reviewing instructions, searching existing data sources, gathering and maintaining the data needed, and completing and reviewing this collection of information. Send comments regarding this burden estimate or any other aspect of this collection of information, including suggestions for reducing this burden to Department of Defense, Washington Headquarters Services, Directorate for Information Operations and Reports (0704-0188), 1215 Jefferson Davis Highway, Suite 1204, Arlington, VA 22202-4302. Respondents should be aware that notwithstanding any other provision of law, no person shall be subject to any penalty for failing to comply with a collection of information if it does not display a currently valid OMB control number. **PLEASE DO NOT RETURN YOUR FORM TO THE ABOVE ADDRESS.**

<b>1. REPORT DATE</b> October 2016		<b>2. REPORT TYPE</b> Annual		<b>3. DATES COVERED</b> 9/30/2015-9/29/2016	
<b>4. TITLE AND SUBTITLE</b> Targeting GPR30 in Abiraterone- and MDV3100-Resistant Prostate Cancer				<b>5a. CONTRACT NUMBER</b>	
				<b>5b. GRANT NUMBER</b> W81XWH-14-1-0271	
				<b>5c. PROGRAM ELEMENT NUMBER</b>	
<b>6. AUTHOR(S)</b> Hung-Ming Lam  E-Mail: minglam@uw.edu				<b>5d. PROJECT NUMBER</b> 0010505049	
				<b>5e. TASK NUMBER</b>	
				<b>5f. WORK UNIT NUMBER</b>	
<b>7. PERFORMING ORGANIZATION NAME(S) AND ADDRESS(ES)</b>  University of Washington 1959 NE Pacific St Seattle WA98195				<b>8. PERFORMING ORGANIZATION REPORT NUMBER</b>	
<b>9. SPONSORING / MONITORING AGENCY NAME(S) AND ADDRESS(ES)</b>  U.S. Army Medical Research and Materiel Command Fort Detrick, Maryland 21702-5012				<b>10. SPONSOR/MONITOR'S ACRONYM(S)</b>	
				<b>11. SPONSOR/MONITOR'S REPORT NUMBER(S)</b>	
<b>12. DISTRIBUTION / AVAILABILITY STATEMENT</b>  Approved for Public Release; Distribution Unlimited					
<b>13. SUPPLEMENTARY NOTES</b>					
<b>14. ABSTRACT</b> Little information is available on the novel treatment for abiraterone (Abi)- and MDV3100 (MDV)-resistant disease. G protein-coupled receptor 30 (GPR30) is a seven-transmembrane estrogen receptor and activation by its specific agonist G-1 inhibited growth in multiple castration-resistant prostate cancer (CRPC) xenograft models that were resistant to the first-generation androgen deprivation therapy. More importantly, GPR30 is an androgen-repressed target and its expression increased in clinical CRPC when compared to primary prostate cancer. Here, we showed that G-1 significantly inhibited the growth and extended the progression-free survival of patient-derived xenograft models that are sensitive (LuCaP 136CR, P=0.046) or minimally responsive to Abi and MDV (LuCaP 35CR, P=0.005). Interestingly, no survival benefit was observed with G-1 when these mice had been pre-treated with Abi or MDV. However, G-1 delayed the development of Abi resistance in the Abi-sensitive LuCaP 136CR, suggesting a defined window for the G-1 therapy. Together with our previous findings, G-1 invariably inhibited 5 models of CRPC, independent of their sensitivity to Abi or MDV. No adverse side effect of G-1 was detected in these preclinical studies. Clinically, GPR30 expression was detected in >90% of CRPC metastases, whereas 80% showed a moderate to high expression level. In rapid autopsy patients who were treated with Abi- and/or MDV, GPR30 was highly expressed in both lung and bone metastases. The high level of GPR30 in CRPC receiving Abi and MDV highlights the potential in effective G-1 therapy on CRPC either in combination with Abi, or on CRPC that is minimally responsive to Abi and MDV.					
<b>15. SUBJECT TERMS</b> Prostate Cancer, Abiraterone, MDV3100, GPR30, Estrogen receptor, G-1, Patient derived xenografts, Treatment resistance					
<b>16. SECURITY CLASSIFICATION OF:</b>			<b>17. LIMITATION OF ABSTRACT</b>	<b>18. NUMBER OF PAGES</b>	<b>19a. NAME OF RESPONSIBLE PERSON</b> USAMRMC
<b>a. REPORT</b>	<b>b. ABSTRACT</b>	<b>c. THIS PAGE</b>			<b>19b. TELEPHONE NUMBER</b> (include area code)
			Unclassified	36	

## Table of Contents

	<b>Page</b>
<b>1. ABSTRACT</b>	4
<b>2. INTRODUCTION</b>	5
<b>3. KEYWORDS</b>	5
<b>4. ACCOMPLISHMENTS</b>	60
<b>5. IMPACT</b>	11
<b>6. CHANGES/PROBLEMS</b>	11
<b>7. PRODUCTS</b>	11
<b>8. PARTICIPANTS AND OTHER COLLABORATING ORGANIZATIONS</b>	11
<b>9. SPECIAL REPORTING REQUIREMENTS</b>	12
<b>10. APPENDICES</b>	12

## 1. ABSTRACT

Targeting GPR30 in Abiraterone- and MDV3100-Resistant Prostate Cancer

Tseona O, Nguyen HM, Heide J, de Frates R, Morrissey C, Corey E, Vessella RL, Lam HM

Department of Urology, University of Washington, 1959 Pacific Street, Seattle, WA 98195

Period 9/30/15-9/29/16

Little information is available on the novel treatment for abiraterone (Abi)- and MDV3100 (MDV)-resistant disease. G protein-coupled receptor 30 (GPR30) is a seven-transmembrane estrogen receptor and activation by its specific agonist G-1 inhibited growth in multiple castration-resistant prostate cancer (CRPC) xenograft models that were resistant to the first-generation androgen deprivation therapy. More importantly, GPR30 is an androgen-repressed target and its expression increased in clinical CRPC when compared to primary prostate cancer. Here, we showed that G-1 significantly inhibited the growth and extended the progression-free survival of patient-derived xenograft models that are sensitive (LuCaP 136CR,  $P=0.046$ ) or minimally responsive to Abi and MDV (LuCaP 35CR,  $P=0.005$ ). Interestingly, no survival benefit was observed with G-1 when these mice had been pre-treated with Abi or MDV. However, G-1 delayed the development of Abi resistance in the Abi-sensitive LuCaP 136CR, suggesting a defined window for the G-1 therapy. Together with our previous findings, G-1 invariably inhibited 5 models of CRPC, independent of their sensitivity to Abi or MDV. No adverse side effect of G-1 was detected in these preclinical studies. Clinically, GPR30 expression was detected in >90% of CRPC metastases, whereas 80% showed a moderate to high expression level. In rapid autopsy patients who were treated with Abi- and/or MDV, GPR30 was highly expressed in both lung and bone metastases. The high level of GPR30 in CRPC receiving Abi and MDV highlights the potential in effective G-1 therapy on CRPC either in combination with Abi, or on CRPC that is minimally responsive to Abi and MDV.

## **2. INTRODUCTION**

Castration-resistant prostate cancer (CRPC) is evolving fast and developing resistance to the most recent treatments including abiraterone (Abi) and MDV3100 (MDV). Treatments to these newly resistant tumors have not been explored. While research efforts continue to abolish the residue androgen signaling in these resistant cells, we propose to focus on androgen-repressed therapeutic targets whose expression is now high under the ultra-low androgen milieu in Abi- and MDV-resistant cancer. G protein-coupled receptor 30 (GPR30) is a seven-transmembrane estrogen receptor and it elicits cell growth or death depending on the cellular context. We showed GPR30 activation by its specific agonist G-1 inhibited prostate cancer growth through G2 arrest and apoptosis. We further showed that GPR30 expression was suppressed by androgen and importantly its expression was increased in castration-resistant prostate cancer (CRPC) in both preclinical setting and clinical specimens. G-1 inhibited the growth of multiple CRPC xenografts that were resistant to the first-generation ADT (i.e. castration). We hypothesize that for CRPC resistant to the second-generation ADT including Abi and MDV, the expression of the androgen-suppressed target GPR30 is high, and hence the anti-tumor effect of G-1 will be maximized.

In this proposal, we will perform preclinical testing on the efficacy and the safety of the GPR30-targeted therapy in our newly developed Abi- and MDV-resistant patient-derived xenografts, and investigate the frequency of GPR30 expression in patient specimens. This study will also provide information on the mechanism underlying GPR30 responsiveness and resistance.

## **3. KEYWORDS**

Prostate Cancer, Abiraterone, MDV3100, GPR30, Estrogen receptor, G-1, Patient derived xenografts, Treatment resistance

## 4. ACCOMPLISHMENTS

### 4.1. G-1 inhibited the growth of CRPC in the absence of prior Abi and MDV treatment

G-1 invariably inhibited growth of 5 CRPC models including LNCaP, C4-2, PC-3 (Lam et al, Endocrine-related Cancer, 2014), LuCaP 136CR, and LuCaP 35CR (**Figure 1**). We completed the G-1 efficacy studies on the growth inhibition in abiraterone (Abi)- and MDV3100 (MDV)-resistant LuCaP xenografts. In both LuCaP 35CR and LuCaP 86.2, tumors took more than expected (take rate 78% and 83%, respectively). The mice were treated with Abi or MDV and resistance to drugs developed as anticipated (**Figure 2**). No weight loss due to treatment was detected (**Figure 3**). Tumor growth was monitored twice weekly. Although G-1 inhibited growth of CRPC, regardless whether the model that are minimally responsive to Abi (LuCaP 35CR) or have acquired resistance to Abi (LuCaP 136CR, **Figure 1**), G-1 did not inhibit growth of CRPC once they received prior treatment with Abi (**Figure 4**) and MDV (**Figure 5**).

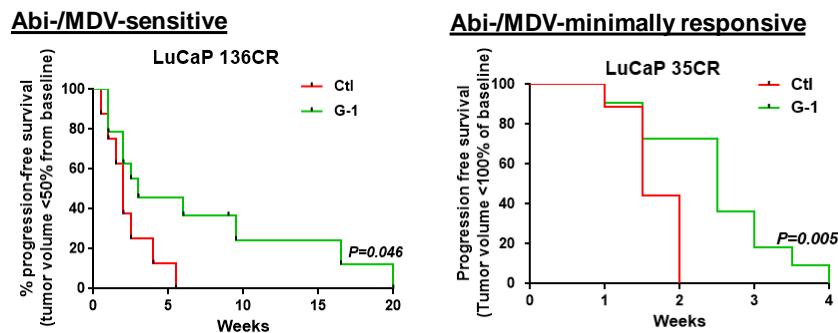


**Figure 1.** G-1 delayed progression in both Abi/MDV – sensitive and – minimally responsive CRPC.

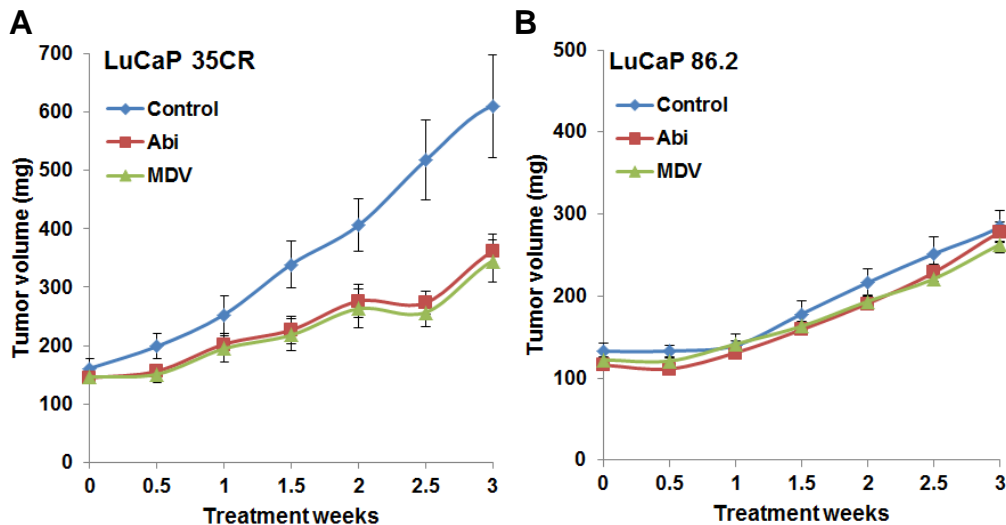


**Figure 2.** Tumor growth upon Abi and MDV resistance in **A**) LuCaP 35CR and **B**) LuCaP 86.2 patient-derived prostate cancer xenografts. Control, n=9; Abi, n=29-40 due to the rolling enrollment; MDV, n=21-37 due to the rolling enrollment.

Next, we evaluated the tumor characteristics associated with G-1 treatment in Abi- and MDV-resistant CRPC. G-1 did not generally alter proliferation except it induced a slight increase in proliferation in LuCaP 136CR ( $P < 0.01$ ) upon Abi resistance, suggesting a tumor model specific induction of proliferation upon G-1 resistance (**Figure 6**). G-1 inhibited apoptosis in LuCaP 136CR and LuCaP 35CR ( $P = 0.02$  and  $P = 0.09$ , respectively), but had no effect on apoptosis in LuCaP 86.2 upon Abi resistance (**Figure 7**). In contrast, G-1 increased apoptosis in LuCaP 86.2 ( $P = 0.01$ ) upon MDV resistance (**Figure 7**). Finally, G-1 treatment did not alter the number of CD34+ blood vessels in Abi- and MDV-resistant CRPCs, suggesting G-1 had no detectable effects on angiogenesis in these CRPC

models (Figure 8). Interestingly, we noticed for the first time that MDV inhibited angiogenesis in both LuCaP 35CR and LuCaP 86.2 (Figure 8;  $P=0.08$  and  $P=0.03$ , respectively), arguing that MDV-resistant tumor may develop mechanisms to survive under a nutrient-deprived environment.

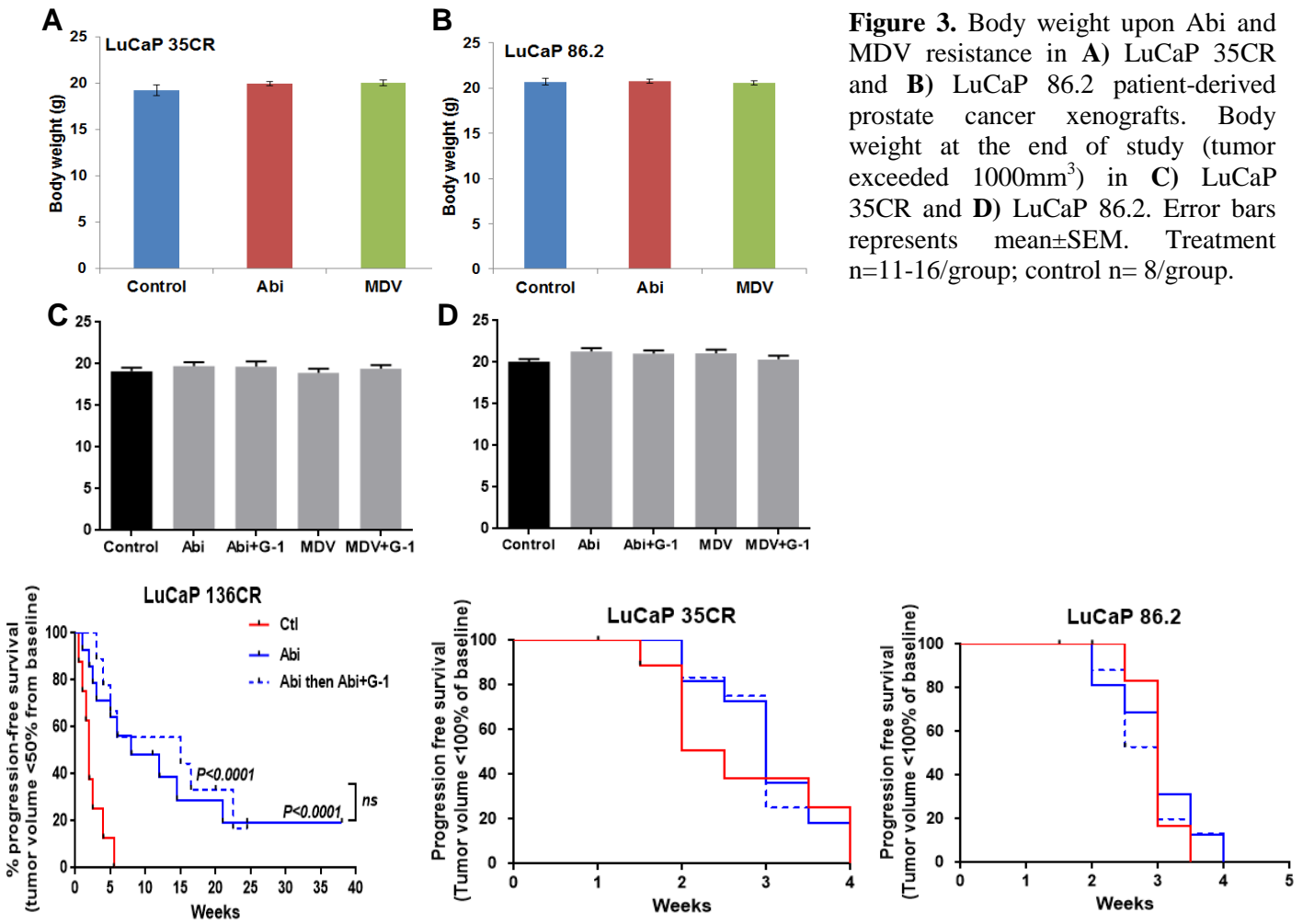


**Figure 4.** G-1 did not delay progression of PDXs that exhibited *de novo* or acquired resistant to Abi.

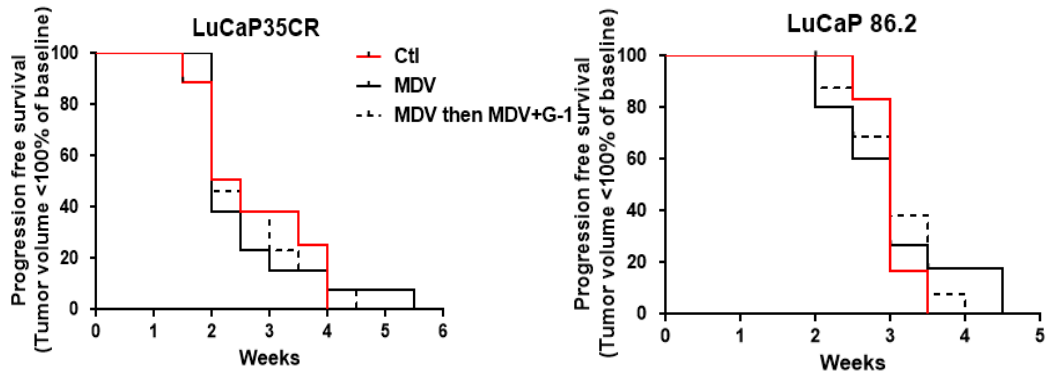


**Figure 5.** G-1 did not delay progression of MDV-resistant PDXs.

## Ki67

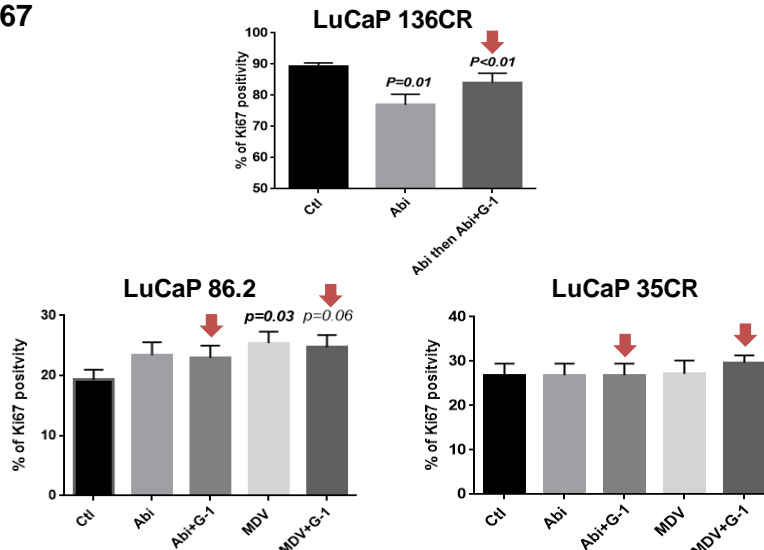


**Figure 6.** G-1 did not alter proliferation upon Abi and MDV resistance, except a slight increase in proliferation was detected in LuCaP 136CR.

## Cleaved caspase-3

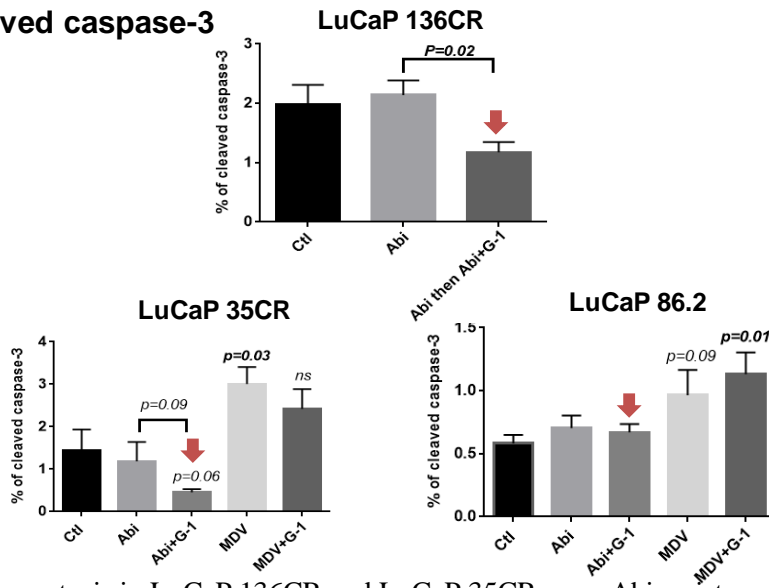


**Figure 7.** G-1 inhibited apoptosis in LuCaP 136CR and LuCaP 35CR upon Abi resistance. G-1 increased apoptosis in LuCaP 86.2 upon MDV resistance.

## CD34

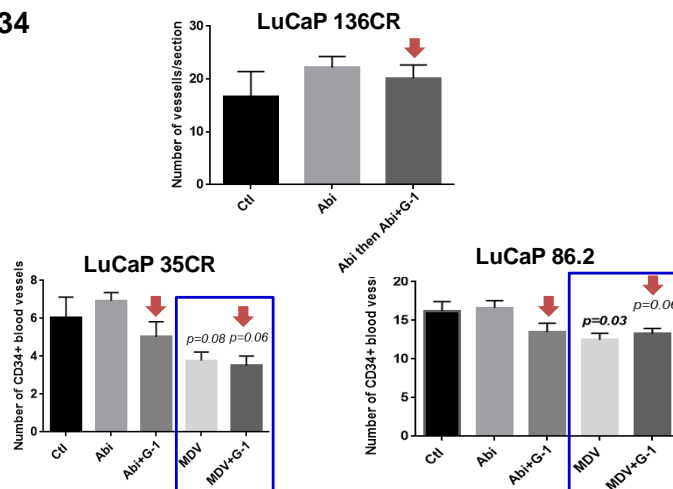


**Figure 8.** MDV inhibited angiogenesis in LuCaP 86.2. G-1 did not alter angiogenesis upon Abi and MDV resistance.

#### 4.2. G-1 delayed Abi resistance and the rate of *de novo* resistance is low in G-1 and Abi combination treatment

G-1 inhibited growth of CRPC but was not able to delay progression in CRPC that acquired resistance to Abi and MDV, therefore we attempted to introduce G-1 earlier in the treatment course by combining Abi and G-1 to investigate if G-1 can delay the development of Abi resistance. In **Figure 9**, G-1 delayed Abi resistance in both LuCaP 136CR and C4-2 CRPC xenograft models. Most importantly, the *de novo* resistance rate to Abi+G-1 combination treatment is very low (8% compared to 43-50% for Abi or G-1 single treatment; **Table 1**). Gene expression studies will be conducted to determine the mechanisms underlying response and resistance mechanism to G-1 on Abi.

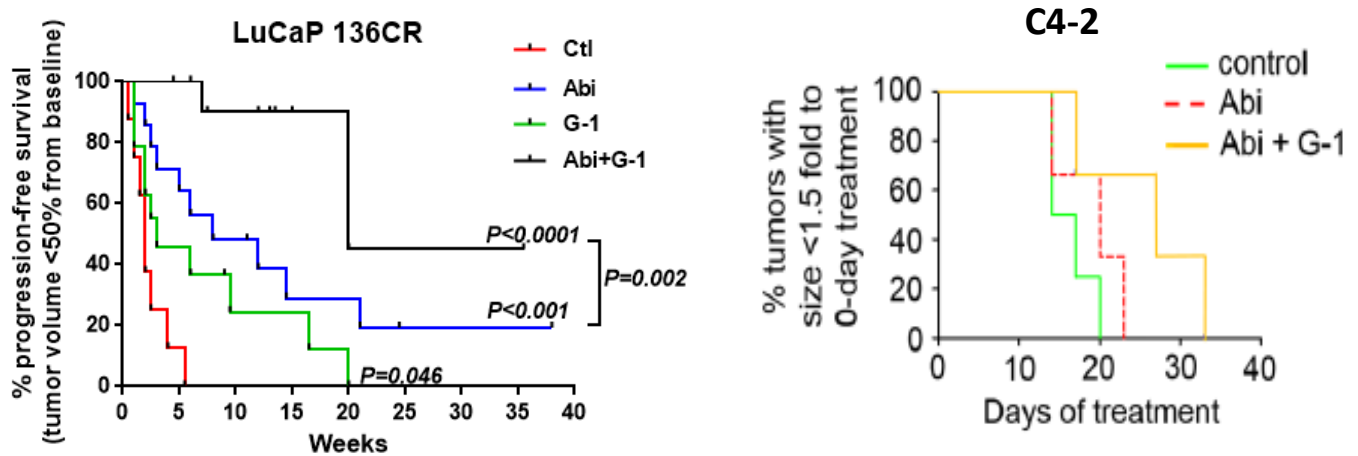


**Figure 9.** G-1 in combination with Abi delayed CRPC progression in LuCaP 136CR and C4-2.

**Table 1.** *De novo* resistance rate is low in G-1 and Abi combination treatment

Treatment	* <i>De novo</i> resistance/total # of animals (%)
Control	8/8 (100%)
Abi	6/14 (43%)
G-1	7/14 (50%)
Abi+G-1	1/12 (8%)

\**De novo* resistance is defined by tumor progression >50% from baseline at 6 weeks of treatment

#### 4.3. GPR30 expression is high in clinical CRPC metastases treated with Abi and MDV

In collaboration with Dr. Bruce Montgomery at the University of Washington, we finished collecting post-Abi biopsies from 30 patients. We also performed 12 rapid autopsies as anticipated. From the rapid autopsy, 5/12 patients had been treated with Abi only, 2/12 with MDV only, and 5/12 with both Abi and MDV. We performed immunohistochemistry staining of GPR30 and found high levels of GPR30 in both bone and soft tissue metastases (including lymph node, lung, and liver) in the patients who received Abi and/or MDV treatment (**Figures 10 and 11**). Comparing between CRPC metastases from patients who had expired in the pre- and post-Abi/MDV era, we found that in the absence of Abi/MDV treatment, GPR30 expression was detected in >90% of CRPC metastases, whereas 80% showed a moderate to high expression level (**Figure 10, upper panel**). In the recent patients who had received Abi and/or MDV, GPR30 expression remained high in both bone and soft tissue metastases in 92% of these patients (**Figure 10, lower panel**). Collectively, the consistent high level of GPR30 expression in CRPC metastasis upon treatment with Abi and/or MDV, and the effective growth inhibition of G-1 in combination with Abi highlighted the potential for an effective combination therapy of Abi+G-1 in >90% of patients. Since GPR30 is an androgen-repressed target, we are preparing samples from the



## 5. IMPACT

### Impact on the development of the principal discipline of the project

Nothing to report

### Impact on other disciplines

Nothing to report

### Impact on technology transfer

Nothing to report

### Impact on society beyond science and technology

Nothing to report

## 6. CHANGES/PROBLEMS

Nothing to report

## 7. PRODUCTS

### Publications, conference papers, and presentations

1. *Targeting estrogen receptors in castration-resistant prostate cancer*, lecture at Prostate Cancer Foundation 22nd Scientific Retreat, Washington DC. October 2015.
2. *Characterization of the abiraterone ultrasponder in castration-resistant prostate cancer*, lecture at Pacific NW Prostate Cancer SPORE Meeting, Seattle, WA. March 2016.
3. *Targeting GPR30 in abiraterone- and MDV3100-resistant prostate cancer*, lecture at DoD PCRP IMPaCT meeting, Towson, MD. August 2016.
4. Tseona O., Nguyen H.M., Heide J., de Frates R., Morrissey C., Corey E., Lam H.M., "Targeting GPR30 in Abiraterone- and MDV3100-resistant Prostate Cancer", poster at DoD PCRP IMPaCT meeting, Towson, MD. August 2016.

## 8. PARTICIPANTS AND OTHER COLLABORATING ORGANIZATIONS

<b>Name</b>	Hung-Ming Lam
<b>Project role</b>	PD/PI
<b>Nearest person month worked</b>	2
<b>Contribution to project</b>	Prepare documents for IACUC, ACURO, and HRPO approvals, and IRB exemptions; design and oversee preclinical studies; analyze and interpret results; clear documents required for abiraterone acetate and MDV3100 transfer

<b>Name</b>	Olena Tseona
<b>Project role</b>	Research scientist
<b>Nearest person month worked</b>	4
<b>Contribution to project</b>	Conduct tumor characterization experiments including tissue sectioning, and immunohistochemistry staining and quantification; acquire abiraterone- and MDV3100-resistant specimens in the prostate cancer rapid autopsy program; prepare tissue microarray and stain for GPR30 in rapid autopsy specimens; extract RNA for gene expression analysis.

<b>Name</b>	Jessica Olson
<b>Project role</b>	Research scientist
<b>Nearest person month worked</b>	2
<b>Contribution to project</b>	Perform preclinical studies including castration of the mouse, tumor

	inoculation, tumor measurement, drug administration, PSA measurement, mouse sacrifice, and tissue acquisition; acquire abiraterone- and MDV3100-resistant specimens in the prostate cancer rapid autopsy program
--	--

<b>Name</b>	Holly Nguyen
<b>Project role</b>	Research scientist
<b>Nearest person month worked</b>	2
<b>Contribution to project</b>	Submit IACUC protocol; perform preclinical studies and organize results; acquire abiraterone- and MDV3100-resistant specimens in the prostate cancer rapid autopsy program
<b>Funding support</b>	NIH/NCI

**Changes in active support**

Nothing to report

**Other organizations involved as partners**

<b>Organization name</b>	Janssen Pharmaceuticals
<b>Location of organization</b>	Raritan, NJ
<b>Contribution to the project</b>	Provided abiraterone acetate for the study

<b>Organization name</b>	Astell/Medivation
<b>Location of organization</b>	San Francisco, CA
<b>Contribution to the project</b>	Provided MDV3100 for the study

**9. SPECIAL REPORTING REQUIREMENTS**

N/A

**10. APPENDICES**

Next page

# Targeting GPR30 with G-1: a new therapeutic target for castration-resistant prostate cancer

Hung-Ming Lam<sup>1,†</sup>, Bin Ouyang<sup>1</sup>, Jing Chen<sup>1</sup>, Jun Ying<sup>1</sup>, Jiang Wang<sup>2</sup>, Chin-Lee Wu<sup>3</sup>,  
Li Jia<sup>4,‡</sup>, Mario Medvedovic<sup>1,5</sup>, Robert L Vessella<sup>6</sup> and Shuk-Mei Ho<sup>1,5,7,8</sup>

<sup>1</sup>Department of Environmental Health, University of Cincinnati Medical Center, Room 128 Kettering Complex, Cincinnati, Ohio 45267-0056, USA

<sup>2</sup>Department of Pathology and Laboratory Medicine, University of Cincinnati Medical Center, Cincinnati, Ohio, USA

<sup>3</sup>Department of Pathology, Massachusetts General Hospital and Harvard Medical School, Boston, Massachusetts, USA

<sup>4</sup>Department of Medicine, Center for Pharmacogenomics, Washington University School of Medicine, St Louis, Missouri, USA

<sup>5</sup>Center for Environmental Genetics, University of Cincinnati Medical Center, Cincinnati, Ohio, USA

<sup>6</sup>Department of Urology, University of Washington, Seattle, Washington, USA

<sup>7</sup>Cincinnati Veterans Affairs Medical Center, Cincinnati, Ohio, USA

<sup>8</sup>Cincinnati Cancer Center, Cincinnati, Ohio, USA

<sup>†</sup>H-M Lam is now at Department of Urology, University of Washington, Box 356510, Seattle, Washington 98195, USA

<sup>‡</sup>L Jia is now at Division of Urology, Department of Surgery, Brigham and Women's Hospital, Boston, Massachusetts 02115, USA

Correspondence  
should be addressed  
to S-M Ho  
**Email**  
Shuk-mei.Ho@uc.edu

## Abstract

Castration-resistant prostate cancer (CRPC) is an advanced-stage prostate cancer (PC) associated with high mortality. We reported that G-1, a selective agonist of G protein-coupled receptor 30 (GPR30), inhibited PC cell growth by inducing G2 cell cycle arrest and arrested PC-3 xenograft growth. However, the therapeutic actions of G-1 and their relationships with androgen *in vivo* are unclear. Using the LNCaP xenograft to model PC growth during the androgen-sensitive (AS) versus the castration-resistant (CR) phase, we found that G-1 inhibited growth of CR but not AS tumors with no observable toxicity to the host. Substantial necrosis (approximately 65%) accompanied by marked intratumoral infiltration of neutrophils was observed only in CR tumors. Global transcriptome profiling of human genes identified 99 differentially expressed genes with 'interplay between innate and adaptive immune responses' as the top pathway. Quantitative PCR confirmed upregulation of neutrophil-related chemokines and inflammation-mediated cytokines only in the G-1-treated CR tumors. Expression of murine neutrophil-related cytokines also was elevated in these tumors. *GPR30* (*GPER1*) expression was significantly higher in CR tumors than in AS tumors. In cell-based experiments, androgen repressed *GPR30* expression, a response reversible by anti-androgen or siRNA-induced androgen receptor silencing. Finally, in clinical specimens, 80% of CRPC metastases ( $n=123$ ) expressed a high level of GPR30, whereas only 54% of the primary PCs ( $n=232$ ) showed high GPR30 expression. Together, these results provide the first evidence, to our knowledge, that GPR30 is an androgen-repressed target and G-1 mediates the anti-tumor effect via

## Key Words

- ▶ androgen deprivation therapy
- ▶ androgen-repressed gene
- ▶ metastases
- ▶ tumor-infiltrating neutrophils

neutrophil-infiltration-associated necrosis in CRPC. Additional studies are warranted to firmly establish GPR30 as a therapeutic target in CRPC.

Endocrine-Related Cancer  
(2014) 21, 903–914

## Introduction

Androgen ablation therapies are mainstay treatments for advanced prostate cancer (PC; Tannock *et al.* 2004, Higano *et al.* 2009, de Bono *et al.* 2011). Unfortunately, almost all patients ultimately fail to respond to these therapies and develop castration-resistant PC (CRPC) that grows in the presence of castration levels of circulating testosterone (de Bono *et al.* 2011). Although chemotherapy (docetaxel or cabazitaxel; Tannock *et al.* 2004, de Bono *et al.* 2010), immunotherapy (e.g. sipuleucel-T; Higano *et al.* 2009, Kantoff *et al.* 2010), or complete androgen blockade (e.g. abiraterone; de Bono *et al.* 2011) may extend the lives of some patients, these treatments all have documented side effects and a relatively short duration of response. Hence, the development of new CRPC therapies with durable efficacy and low toxicity is warranted.

Estrogens have a long history of efficacy for advanced PC (Oh 2002). Huggins & Hodges (2002) first reported the use of diethylstilbestrol for advanced PC in 1941. However, severe cardiovascular toxicity of oral estrogens limited their use in PC (Norman *et al.* 2008). The early efficacy of parenteral estrogen in recent studies (Schellhammer 2012, Langley *et al.* 2013) and especially the better toxicity profiles owing to hepatic bypass (Norman *et al.* 2008) reinvigorated interest in the use of estrogens as a therapy for PC. In addition to the suppression of testosterone effects by estrogens, estrogens are also directly cytotoxic to PC cells (Ho *et al.* 2011). The actions of parenteral estrogens are believed to be mediated by the classical estrogen receptors (ERs), ESR1 and ESR2. However, the exact effects of the two ERs and their isoforms on PC growth and metastases may vary according to cellular contexts (Claessens & Tilley 2014, Nelson *et al.* 2014). We have recently reported that G-1 (1(1-(4-(6-bromobenzo(1,3)dioxol-5-yl)-3a,4,5,9b-tetrahydro-3H-cyclopenta(c)quinolin-8-yl)-ethanone)), which selectively activates the third ER, G protein-coupled receptor 30 (GPR30 or GPER) (Bologa *et al.* 2006), inhibited the growth of multiple PC cell lines and PC-3 xenografts, and exerted few or no adverse effects on the animals (Chan *et al.* 2010). These results indicate that G-1, by targeting GPR30, might offer a new treatment option for PC.

GPR30 is structurally unrelated to the classical ERs (ESR1 and ESR2). It is a seven-transmembrane-domain receptor localized at the cell surface (Bologa *et al.* 2006, Funakoshi *et al.* 2006), endoplasmic reticulum (Thomas *et al.* 2005, Prossnitz *et al.* 2007, Otto *et al.* 2008), perinuclear compartment (Cheng *et al.* 2011), and nucleus (Madeo & Maggiolini 2010). The successful development of a highly selective non-steroidal agonist, G-1, for GPR30, provides a tool for studying the action of GPR30 independent of the actions mediated by ESR1 and ESR2 (Bologa *et al.* 2006, Blasko *et al.* 2009). Activation of GPR30 was found to play opposite roles in the regulation of the growth of various normal and neoplastic tissues, promoting growth of breast, endometrium, and ovarian tissues (Filardo *et al.* 2000, Vivacqua *et al.* 2006, Albanito *et al.* 2007, Pandey *et al.* 2009), but inhibiting growth of thymocytes, urothelial cells, vascular smooth muscle cells, and ER-positive breast cancer cells (Albanito *et al.* 2007). The dual action of GPR30 could be related in part to its differential activation of downstream mediators, including EGFR, PI3K, Erk1/2, cAMP, and intracellular Ca<sup>2+</sup> (reviewed in Maggiolini & Picard (2010) and Prossnitz & Barton (2011)). We demonstrated that in PC cells, the activation of GPR30 by G-1 leads to growth inhibition via an ERK/p21-mediated cell cycle arrest at the G2 phase (Chan *et al.* 2010). In addition, we found that G-1 inhibited the growth of PC-3 xenografts that lack the androgen receptor (AR). Still unknown are the mode of action of G-1 *in vivo* and the potential link between its efficacy and androgen status in PC.

This study evaluated the efficacy of G-1 in inhibiting the growth of LNCaP xenografts during the androgen-sensitive (AS) or the castration-resistant (CR) phase. In this study, we report that G-1 inhibited the growth of the xenograft in castrated (low testosterone) animals but not in intact, androgen-supported animals (high testosterone). The G-1-induced growth inhibition in the CR xenograft was associated with massive necrosis, neutrophil infiltration, upregulation of a set of cell-mediated immune response genes, and enhanced expression of *GPR30* (*GPER1*). Results obtained from cell-based experiments revealed that *GPR30* is repressed by androgen,

whereas immunohistochemical results indicated a larger proportion of human CRPC metastases than primary PC express high GPR30 level. Collectively, these results provide support for targeting GPR30 with G-1 as a possible new approach for the treatment of CRPC.

## Materials and methods

### Human specimens

Human tissue microarrays were obtained from Massachusetts General Hospital (primary PC) and the University of Washington (metastatic CRPC). Samples were de-identified; only those with complete clinical information, follow-up data, and good tissue quality were included. The primary PC cohort comprised one specimen each from 232 patients with PC (i.e. 232 specimens) taken at prostatectomy (Leung *et al.* 2010). The metastatic CRPC cohort comprised patients who participated in the Rapid Autopsy Program during the period 1999–2006; it consisted of 123 CRPC specimens, including 75 bone (spine, ribs, pelvis, sternum, ischium, iliac, and sacrum), 29 lymph node, 14 liver, and five lung metastasis tissues from 24 patients. The use of the specimens was reviewed and approved by the Institutional Review Board committees of the respective universities.

### Cell culture and siRNA experiments

Human PC cell lines LNCaP and PC-3 were obtained from the American Type Culture Collection (ATCC, Manassas, VA, USA) and passaged for less than 3 months after resuscitation. Both LNCaP and PC-3 were retro-authenticated by ATCC with short tandem repeat profiling (March 13, 2013) and confirmed to be the original cell line. LNCaP cells were maintained in RPMI-1640 medium (Invitrogen) supplemented with 10% FBS; sodium pyruvate, 1 mmol/l; L-glutamine, 2 mmol/l; and D-glucose, 1.25 g/l. PC-3 cells were maintained in F-12K medium (ATCC) supplemented with 10% FBS. Cells were cultured at 37 °C in an atmosphere of 5% CO<sub>2</sub>. For androgen treatment (R1881 and dihydrotestosterone (DHT)), LNCaP ( $2.5 \times 10^5$ ) and PC-3 ( $2 \times 10^5$ ) cells were seeded in phenol-red-free RPMI-1640 (with supplements) and F-12K media, respectively, supplemented with 10% charcoal-stripped FBS. For drug treatment, drugs were added daily for 4 days, and the medium was changed every 2 days. For siRNA-AR (siAR) transfection, cells were replenished with 1.6 ml of fresh medium and 400  $\mu$ l of siAR-DharmaFECT mixture (50 nM Stealth RNAi siAR, Invitrogen; DharmaFECT3 for LNCaP and DharmaFECT2

for PC-3 cells, Dharmacon, Lafayette, CO, USA) the following day. At day 3, cells were recovered with the respective medium containing 10% charcoal-stripped FBS, and drugs were added daily for 4 days. Transfection was repeated on day 2 of drug treatment. At the end of the experiments, cells were collected for RNA extraction. For the transfection-negative control, cells were treated with DharmaFECT and siRNA-non-targeting (siNT, Dharmacon).

### Chromatin immunoprecipitation assay

Chromatin immunoprecipitation (ChIP)-sequencing and ChIP were carried out as described previously using an antibody to AR (ab74272, Abcam, Cambridge, MA, USA; Decker *et al.* 2012). The site-specific qPCR primers for the AR-binding site at the *GPER1* (*GPR30*) locus were as follows: forward, 5'-CTGGGACAACGTGAGCAGTAAG-3' and, reverse, 5'-CCAACTACTTTACCAGCCAGCA-3'. The primers for prostate-specific antigen (PSA (*KLK3*)) enhancer and control regions have been described previously (Zheng *et al.* 2013).

### Microarray experiment and analysis

RNA was extracted from LNCaP xenografts with TRIzol Reagent (Invitrogen); RNA extracts with integrity numbers of less than 8 (four animals in each group), as measured by Agilent 2100 Bioanalyzer (Agilent, Santa Clara, CA, USA), were used for microarray analysis. The detailed microarray study is available in the [Supplementary Methods](#), see section on [supplementary data](#) given at the end of this article. The data are accessible through the NCBI Gene Expression Omnibus Series accession number: GSE54974.

### Xenograft study

In the first set of experiments, *GPR30* mRNA expression was compared in tumors grown before and after the castration of mice. Male athymic nude mice (4–6 weeks old, 20–25 g, Taconic, Hudson, NY, USA) each received a subcutaneous implant of a 2 cm-long silastic capsule containing ~15 mg testosterone (Sigma), while the animals were under general anesthesia using isoflurane. After 2 days, LNCaP cells ( $5 \times 10^6$  cells) in 150  $\mu$ l of Matrigel (BD Biosciences, Franklin Lakes, NJ, USA) were injected subcutaneously into the flanks of mice, and the tumors that developed were measured twice weekly (Chan *et al.* 2010). When the tumors reached 150–300 mm<sup>3</sup>, mice were divided into two groups: intact and castrated animals. Tumors growing in the intact mice are referred

as AS tumors. For the castrated group, the silastic capsules were removed and mice were surgically castrated under general anesthesia using isoflurane. Tumors regressed and then regrew after castration (approximately 3 weeks post-castration); these tumors are referred as CR. AS or CR tumors at approximately 1000 mm<sup>3</sup> were collected to determine the expression of *GPR30* mRNA.

In the second set of experiments, the therapeutic efficacy of G-1 on AS and CR tumors was evaluated and compared. LNCaP xenografts were developed as described in the first set of experiments. Both AS and CR tumors were enrolled when tumors reach approximately 300–400 mm<sup>3</sup> in size. Mice received subcutaneous injections of a vehicle (95% PBS, 2.5% DMSO, and 2.5% ethanol; v/v) or G-1 (4 mg/kg) daily for 16 days. Tumors and body weight were measured twice weekly. Mice were killed and weighed after removal of the xenografts. The protocol for animal use was approved by the Institutional Animal Care Committee at the University of Cincinnati.

### Serum enzyme assays

Serum obtained from mice was assayed for creatine kinase (CK), lactate dehydrogenase (LDH), alanine transaminase (ALT), and aspartate transaminase (AST) using IDTox enzyme assay kits (ID Labs, London, ON, Canada) following the manufacturer's protocols.

### Quantitative real-time PCR

Total RNA was treated with RNase-free DNase (Qiagen) and reverse-transcribed (Chan *et al.* 2010). Real-time PCR was carried out as described previously (Chan *et al.* 2010). Species-specific primer sequences are presented in [Supplementary Table S1](#), see section on [supplementary data](#) given at the end of this article. PCRs with SYBR GreenER PCR Master-Mix (Invitrogen) were monitored using the 7900HT Fast Real-time PCR System (Applied Biosystems). Individual mRNA levels were normalized to glyceraldehyde-3-phosphate dehydrogenase (*GAPDH*).

### Histopathology and immunohistochemistry analyses

Formalin-fixed xenograft samples were processed for hematoxylin and eosin (H&E) staining and subjected to histological examination for necrosis and inflammation; the thickness of the tumor capsule was determined by the surgical pathologist (J W). Analysis of paraffin-embedded human PC and LNCaP xenograft sections by immunohistochemistry (IHC) was performed as described previously

(Leav *et al.* 2001). Antibodies and quantification of necrosis and markers are described in the [Supplementary Methods and Table S2](#), see section on [supplementary data](#) given at the end of this article.

For clinical specimens, GPR30 expression was graded independently by two investigators (H-M L and J W) in a blinded manner. Signal intensity (0–3) and percentage of signal coverage (0–100) of each section were scored, and the product of the intensity and coverage was represented as an *H*-score (0–300) (Huang *et al.* 2005). For the metastatic CRPC cohort, *H*-scores were an average of duplicated cores in a specified metastatic site of each patient. In all cases of bone metastases, two to three sites were acquired per patient and an average *H*-score was calculated. The distribution of the *H*-score showed bi-modal or multi-modal properties in the clinical data: 45% of the specimens showed *H*-scores of less than 100, approximately 32% of the specimens showed *H*-scores of 100–199 and 23% of the specimens amassed *H*-scores of 200–300. In this study, we used a dichotomous variable of *H*-score group (i.e. *H*-score of 100 or more versus less than 100) in the analysis to reduce possible bias due to the distribution of the original *H*-score and to improve the statistical power. In order to assess the sensitivity of using different definitions to the *H*-score variables, the same analysis was repeated after replacing the dichotomous variable with a three-level category variable (i.e. *H*-score 0–99 versus 100–199 versus 200–300) as well as the original *H*-score. Those results were found to be consistent with the results of the main analysis using the dichotomous variable presented in this study.

### Statistical analyses

Numerical dependent variables were analyzed by one-way ANOVA and the *post hoc* Bonferroni tests to compare means if more than two groups were involved. *t*-tests were used if means of two groups were compared. Categorical dependent variables were compared among groups using  $\chi^2$  tests. All differences were considered significant when  $P < 0.05$ .

## Results

### G-1 inhibits growth and induces necrosis in CR tumors with no apparent toxicity to the host

We compared the inhibitory effect of G-1 on AS or CR tumors growing in intact or castrated (low testosterone) mice respectively. Administration of G-1 significantly

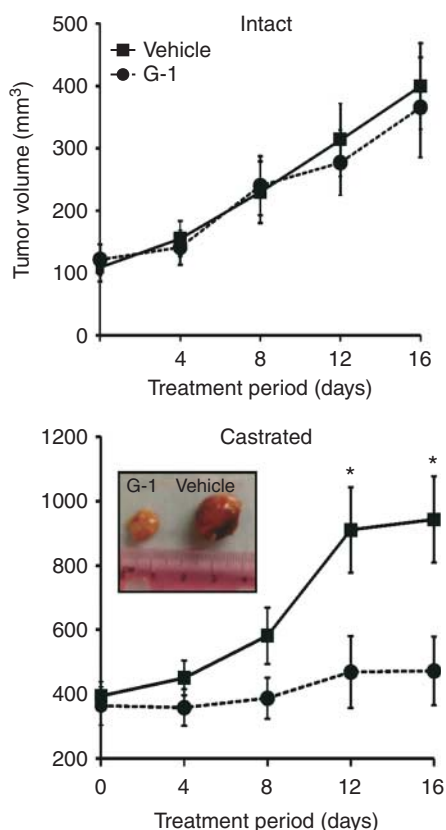


**Figure 1**

G-1 inhibited growth and induced necrosis in the castration-resistant tumors. G-1 inhibited growth of the CR tumor (bottom panel) but not the androgen-sensitive tumors (top panel). When LNCaP xenografts grew to 150 mm<sup>3</sup>, mice were divided into two groups: intact and castrated. Intact animals received subcutaneous injections of a vehicle (2.5% DMSO and 5% ethanol) or G-1 (4 mg/kg) daily for 16 days. For the castrated group, mice were castrated and, when the tumor re-emerged, they were treated with a vehicle or G-1 daily for 16 days. Error bars represent mean  $\pm$  S.E.M.,  $n=6-8$ /group, \* $P<0.05$ .

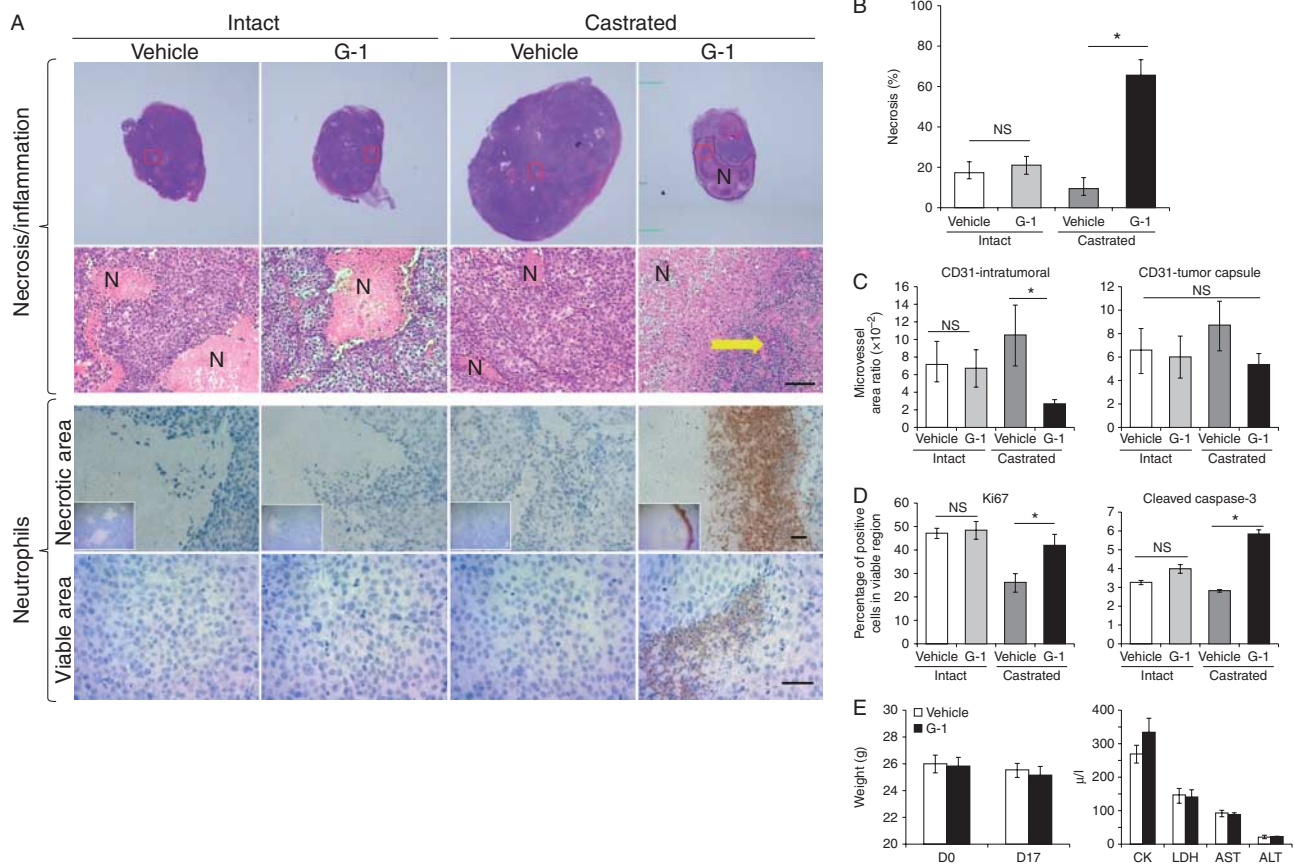
inhibited the growth of CR tumors after 16 days of treatment ( $P<0.05$ , Fig. 1). Similar results were obtained in CR tumors including C4-2 and PC-3 (Supplementary Figure S3, see section on supplementary data given at the end of this article). Massive necrosis and inflammation were observed only in the G-1-treated LNCaP CR tumors (in seven out of eight mice). Inflammation was attended by considerable neutrophil infiltration of the necrotic area as well as of the healthy area of these tumors (Fig. 2A). This intratumoral neutrophil infiltration was not observed in either vehicle-treated CR tumors or vehicle/G-1-treated AS tumors that displayed only ischemic necrotic foci with no inflammation/neutrophils (Fig. 2A). We did not examine T cells in this study because nude mice are deficient in these cells (Pelleitier & Montplaisir 1975).

B cells and macrophages were found exclusively in the intratumoral stroma and the tumor capsule, respectively, in all treatment groups (Supplementary Figure S1). Notably, G-1-induced necrosis occupied an average of 65% of the tumor volume ( $P=0.0003$ , Fig. 2B). Furthermore, G-1 significantly reduced the intratumoral microvessel density in CR tumors but not in AS tumors (Fig. 2C, left panel). No significant alteration in microvessel density was observed in the tumor capsule with G-1 treatment (Fig. 2C, right panel). In the viable area of the tumors, cell proliferation (Ki67 staining) remained relatively constant in the four treatment groups except for an increase of 10–20% when compared with vehicle-treated counterparts in Ki67-staining cells in G-1-treated CR tumors (Fig. 2D, left panel). G-1 induced a slight but significant increase in apoptosis (cleaved caspase-3 staining) in the CR tumors (Fig. 2D, right panel).

Our previous work had demonstrated that G-1 did not have general toxicity (on the basis of body weight and tissue histology) in the animals (Chan et al. 2010). In this study, we further report that G-1 did not induce any changes in body weight or cause functional damage to the heart or the liver in mice after 16 days of treatment with G-1, as indicated by the levels of injury biomarkers in the serum (CK and LDH for heart injuries; AST and ALT for liver injuries, Fig. 2E).

### G-1 induced specific changes in gene expression exclusively in CR tumors

Global transcriptome profiling was performed on vehicle/G-1-treated AS and CR tumors (four groups of tumors,  $n=4$ ). Overall, the profiling results identified 2446 differentially expressed genes among the four treatment groups (false discovery rate (FDR)  $<0.1$ ,  $P<0.01$ ,  $n=4$  per group). Unbiased hierarchical clustering analysis showed no significant differences in gene expression between the vehicle-treated and the G-1-treated AS tumors (Fig. 3, left side of heat map). However, this analysis identified two clusters of genes (a total of 1082) that were altered by G-1 exclusively in the CR tumors (Fig. 3, right side of heat map). Subsequent gene shaving using two additional criteria –  $P<0.01$  and a difference of at least 1.5-fold between G-1-treated and vehicle-treated CR tumors – yielded a final set of 99 genes (Fig. 3A, gray panel). Ingenuity Pathway Analysis (IPA) of the 99 genes showed enrichment of the top biological pathway ‘antigen presentation, cell-to-cell signaling and interaction, and inflammatory response’, followed by ‘genetic disorder, neurological disease, and skeletal and muscular disorders’. Furthermore, the top canonical

**Figure 2**

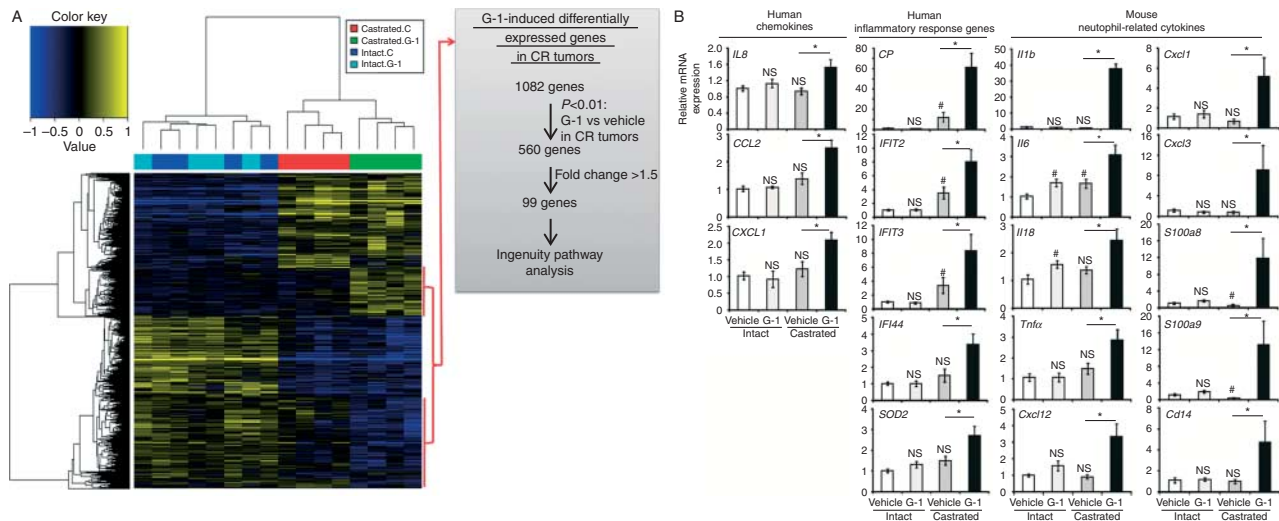
G-1 induced massive necrosis and neutrophil infiltration in the CR tumors. (A) G-1 triggered massive necrosis in CR tumors. Tumor sections were stained with H&E, and the necrotic area was quantified as described in the Supplementary Methods. (B) G-1 induced significant necrosis associated with massive inflammation, which in turn was associated with neutrophil infiltration, both surrounding the necrotic area and within the viable area, in CR tumors only. The yellow arrow represents massive inflammation. Magnification: 20× (H&E, upper panel), 200× (H&E, lower panel), 100× (neutrophil IHC, upper panel), and 200× (neutrophil IHC, lower panel). Scale bars represent 50 μm in all micrographs. (C) G-1 reduced the

microvessel area ratio in the intratumoral stromal region but not in the tumor capsule. Microvessel area ratio is calculated as the ratio of the microvessel area to the intratumoral stromal area or the capsule area. (D) Ki67 and cleaved caspase-3 staining of tumor cells was used to determine proliferation and apoptosis respectively. (E) G-1 did not induce toxicity in castrated mice as determined by the absence of changes in body weight (left panel) and in serum assays of organ damage marker enzymes (right panel). Error bars represent mean ± s.e.m.,  $n=6-8$ /group, \* $P<0.05$ ; NS, not significant; H&E, hematoxylin and eosin; IHC, immunohistochemistry.

pathway identified in this specific set of G-1-associated genes is 'communication between innate and adaptive immune cells' (Supplementary Table S3, see section on supplementary data given at the end of this article).

To focus on identifying molecular mediators of G-1-induced inflammation/neutrophil infiltration, we selected a set of genes from the 99-gene panel for confirmation based on a literature search showing their relatedness to cell-mediated immune responses. Quantitative real-time PCR analyses ( $n=6$  per group) validated the upregulation of the expression of these genes in G-1-treated CR tumors but not in G-1-treated AS tumors when compared with their respective vehicle-treated controls. These include

four chemokine genes *CP*, *IL8* (*CXCL8*), *CCL2*, and *CXCL12*; three interferon-induced antiviral genes *IFIT2*, *IFIT3*, *IFIT4*; and *SOD2*, an important oxidative stress response gene (Fig. 3B). As human interleukin 8 (IL8) is a strong chemo-attractant for both human and mouse neutrophils (Geiser *et al.* 1993, Schaidler *et al.* 2003), we analyzed murine neutrophil-related cytokine genes using quantitative real-time PCR. Expression of murine genes involved in neutrophil movement, accumulation, adhesion, activation, and phagocytic respiratory burst, including *Il1b*, *Il6*, *Il18*, *Tnfa* (*Tnf*), *Cxcl12*, *Cxcl1*, *Cxcl3*, *S100a8*, *S100a9*, and *Cd14* (Cacalano *et al.* 1994, Leung *et al.* 2001, Ryckman *et al.* 2003, Harokopakis &

**Figure 3**

G-1 induced unique changes in gene expression in castrated animals. (A) Heat map of hierarchically clustered differential gene expression in intact or castrated animals treated with a vehicle or G-1 blue, down-regulated; yellow, upregulated;  $n=4$  per group. A scheme for gene selection for Ingenuity Pathway Analysis is shown. (B) Quantitative real-time PCR analyses of the G-1-induced human and mouse genes in

Hajishengallis 2005, Eash *et al.* 2010), was elevated by 1.8- to 50.9-fold in G-1-treated vs vehicle-treated CR tumors (Fig. 3B). Interestingly, the expression of human *IL1B* was not altered in CR tumors with G-1 treatment.

### Androgen represses *GPR30* expression via AR, and castration increases *GPR30* expression

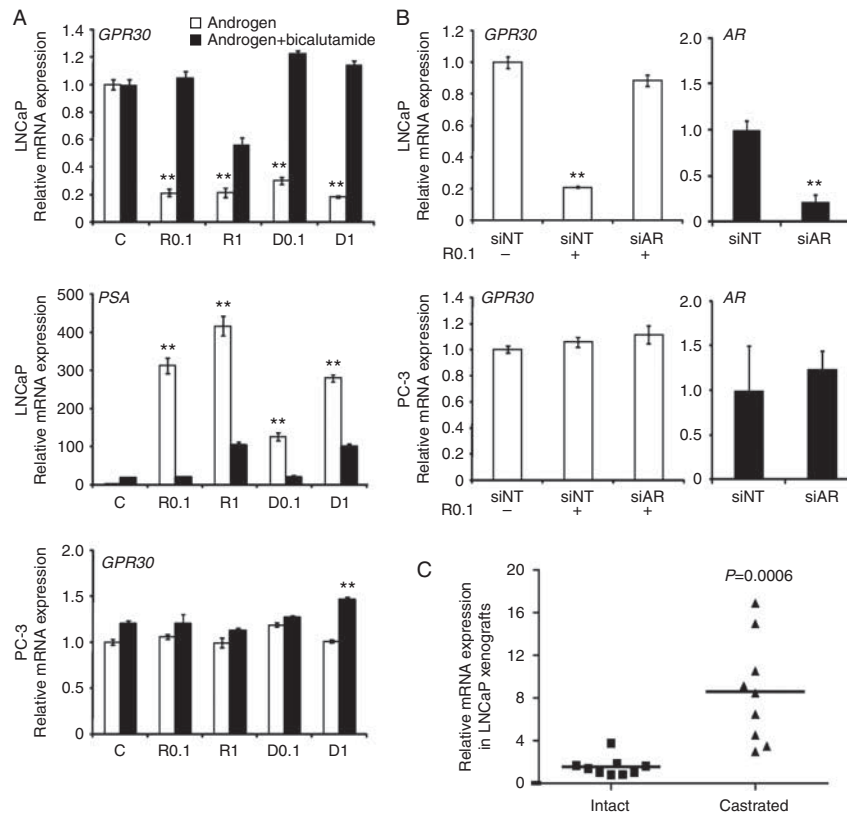
In an attempt to explain why G-1 inhibited growth only in an androgen-deprived environment, we determined the effect of androgen on *GPR30* expression. Androgen is the principal hormone regulating prostate function. Treatment of LNCaP cell cultures with R1881 (a synthetic androgen) or DHT (the physiologically active androgen) reduced the expression of *GPR30* mRNA; the effects of these androgens were abolished by cotreatment with bicalutamide, an AR antagonist, or by transduction of a siRNA against AR (Fig. 4A and B, upper panels). These responses were not observed in the AR-negative PC-3 cells (Fig. 4A and B, bottom panels). These results indicate that androgen represses *GPR30* expression via mechanisms involving the AR. Furthermore, ChIP-sequencing analyses of LNCaP cells revealed a strong AR-binding site approximately 3.5 kb downstream of the 3' end of the *GPR30* (*GPER1*) gene after androgen stimulation (Supplementary Figure S2, see section on supplementary data given at the

end of this article, upper panel). This AR-binding site on *GPR30* was further validated by an independent site-specific ChIP-qPCR analysis (Supplementary Figure S2, lower panel).

In the LNCaP xenograft model, expression of *GPR30* mRNA was significantly higher (approximately eightfold) in CR tumors grown in castrated mice than in AS tumors grown in intact mice (Fig. 4C). Expression of *AR* mRNA in CR tumors was increased by 1.8- to 4.6-fold when compared with that in AS tumors (data not shown). These results are in concordance with those from cell-based studies, indicating that *GPR30* expression is repressed by androgen via AR-mediated signaling.

### *GPR30* expression is higher in metastatic CRPC than in primary PC

We reasoned that *GPR30* in CRPC metastases needs to be expressed at significant levels before we can consider it as a new therapeutic target for CRPC. Hence, we used IHC to assess the level of *GPR30* expression in specimens obtained from two cohorts of patients. The first cohort included only primary cancers from specimens obtained at prostatectomy ( $n=232$ ) and the second comprised CRPC metastases ( $n=123$ ). We found that 80% of the metastatic CRPC specimens expressed high levels of *GPR30*, with an

**Figure 4**

Androgen suppressed GPR30 expression via AR. (A) Androgen (white bars, 0.1 and 1 nM) suppressed GPR30 expression, and suppression was reversed by bicalutamide (black bars) in AR-positive LNCaP cells but not in AR-negative PC-3 cells. Cells were treated with androgen in the presence or absence of bicalutamide for 4 days. Prostate-specific antigen (PSA) was a positive control for the androgen-stimulated AR response gene. (B) siAR abolished the androgen-suppressed GPR30 expression in LNCaP cells.

*H*-score of 100 or more when compared with 54% of primary PC specimens with an *H*-score of 100 or more ( $P=0.001$ ) (Fig. 5).

GPR30 staining in PC was not correlated with age, the Gleason score of primary cancer, final PSA level, type of androgen deprivation therapy (ADT), or duration of ADT (Supplementary Table S4, see section on supplementary data given at the end of this article). Interestingly, no difference in the *H*-scores of GPR30 was observed among the 75 bone metastases obtained from different locations (*H*-score approximately 162–165; pelvis/sternum/ischiu-m/iliac/sacrum versus rib/limb versus spine; Supplementary Table S5).

## Discussion

In this study, we determined that G-1, a GPR30 agonist, inhibited the growth of CR tumors but not during their

preceding AS growth phase, with no detectable toxicity to the host. The G-1-induced growth inhibitory response was manifested as massive necrosis attended by marked neutrophil infiltration in the affected tumors, associated with the activation of gene pathways involved in innate antitumor immunity. We also demonstrated that androgen suppressed GPR30 expression in an AR-dependent manner and that castration markedly upregulated its expression. Clinically, we observed an elevated prevalence of high levels of GPR30 in CRPC metastases when compared with that in primary PC. Taken together, these findings provide evidence for the effective preclinical targeting of GPR30 with G-1 for CRPC.

In this study, we aimed to examine the activation of GPR30 by G-1 in both an androgen-supported (intact) and an androgen-deprived (castrated) environment *in vivo*. We had previously demonstrated that G-1 inhibited growth in cell culture experiments and a hormone-independent PC-3

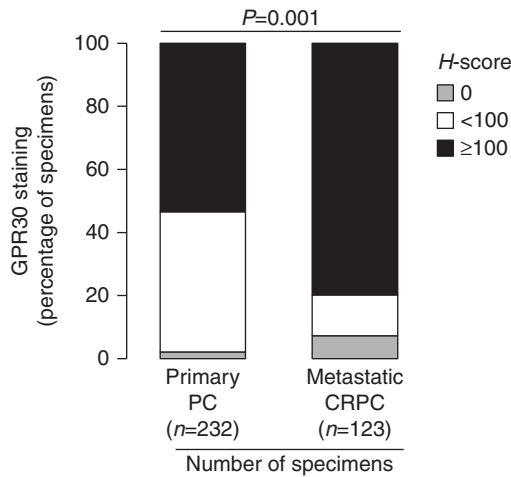


**Figure 5**  
GPR30 staining in primary PC and CRPC metastases. A high level of GPR30 was detected in a larger proportion of metastatic CRPC specimens when compared with primary PC specimens.

xenograft in castrated hosts (Chan *et al.* 2010). This study further demonstrated the efficacy of G-1 in the LNCaP xenograft model, which recapitulates the natural history of PC progression from AS to CR. We found that, in the LNCaP

xenograft model, G-1 inhibited the growth of CR tumors but not AS tumors, indicating that the androgen deprivation may favor the anti-tumor action of G-1.

Histological examinations have indicated that G-1 induced massive tumor necrosis in the castrated mice and invasion of the viable region of G1-treated tumors by numerous tumor-infiltrating neutrophils (TINs). At the molecular level, upregulation of chemokine and inflammatory response genes, including *CP*, *IL8*, *CCL2*, *CXCL12*, and *IFITs*, were uncovered by transcriptome profiling and confirmed by qPCR. Thus, one hypothesis is that chemokines secreted by viable CRPC cells and/or additional tumor tissue remodeling factors stimulated by G-1 may direct the migration of neutrophils (illustrated in Fig. 6). Neutrophils have been implicated in tumor progression and antitumor response. Mild infiltration of neutrophils stimulates proliferation and metastasis in cancer (Gregory & Houghton 2011). However, high levels of TINs induce a destructive oncolytic response (Fu *et al.* 2011) and are associated with cytotoxicity and tumor regression (Di Carlo *et al.* 2001). Neutrophils produce cytotoxic mediators, including reactive oxygen species, proteases, membrane-perforating agents, and soluble cell-kill mediators (Di Carlo *et al.* 2001). Moderate or extensive

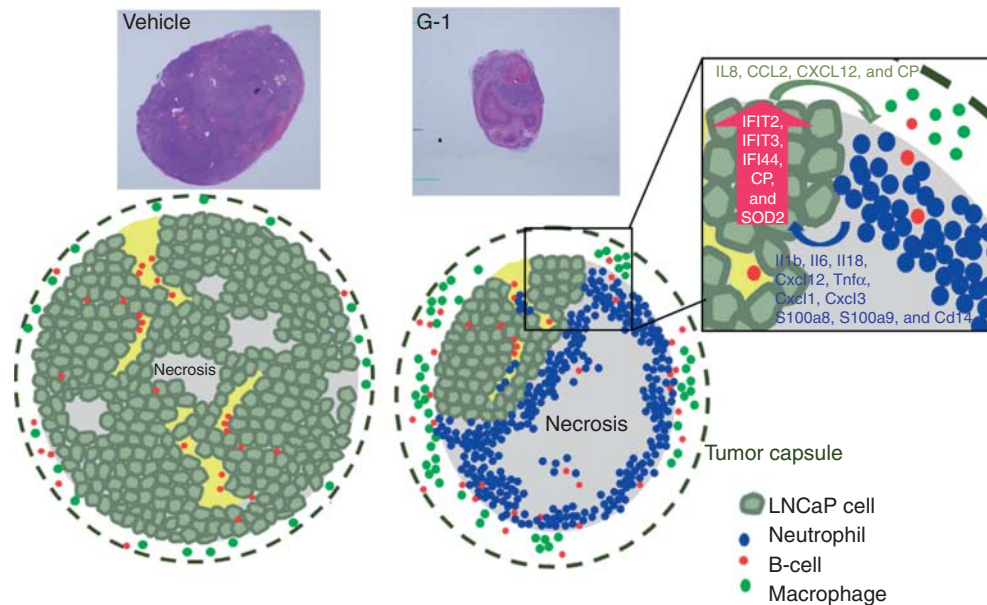


**Figure 6**  
A schematic diagram showing G-1-induced innate antitumor response in castration-resistant LNCaP prostate cancer *in vivo*. For LNCaP xenografts in vehicle- or G-1-treated intact animals or vehicle-treated castrated animals, focal ischemic necrosis was detected in the tumor. However, in G-1-treated castrated animals, massive necrosis and neutrophil infiltration were detected in the necrotic area as well as within the viable area of the tumor.

(Box) In human xenografts, the levels of expression of human-specific chemokine and inflammatory response genes were increased; in the mouse stroma, the levels of expression of a panel of murine-specific neutrophil-related cytokine genes were elevated. In both intact and castrated animals, macrophages resided in the tumor capsule and B cells localized to the intratumoral stroma of the LNCaP xenograft.

levels of TINs are associated with reduced mortality in gastric cancer (Caruso *et al.* 2002), indicating that neutrophils are active in immunosurveillance against cancer. Key TIN-associated cell-kill mediators, including IL1 $\beta$  and tumour necrosis factor alpha (TNF $\alpha$ ) (Di Carlo *et al.* 2001), were detected in the G-1-induced tumor necrosis. Previous results have indicated that transgenic expression of IL8 and TNF $\alpha$  in tumor cells elicited prominent neutrophil-mediated antitumor activity (Hirose *et al.* 1995, Musiani *et al.* 1996). In addition, ceruloplasmin (CP) produced by the CR tumor cells attracts neutrophils and enhances phagocytosis of neutrophils (Saenko *et al.* 1994). In contrast to the systemic upregulation of cytokines, which may pose a health hazard to immunocompromised patients with cancer, local and specific recruitment of neutrophils may provide a new approach to the targeted treatment of cancer (Hirose *et al.* 1995, Fu *et al.* 2011).

GPR30 expression has been reported to be upregulated by various growth factors, HIF1 $\alpha$ , and progesterone (Ahola *et al.* 2002, Albanito *et al.* 2008, Recchia *et al.* 2011, De Marco *et al.* 2013). However, only one report described a decrease in GPR30 expression after estrogen treatment in the human internal mammary artery (Haas *et al.* 2007). This estrogen-induced suppression of GPR30 was not detected in neurons (Jacobi *et al.* 2007), indicating that the regulation of GPR30 expression is cell-context-specific. In this study, we demonstrated for the first time that androgen, the principal hormone in the prostate, inhibited GPR30 expression that was dependent on AR. Interest has started to focus on the crosstalk between AR and ER signaling in PC (Yang *et al.* 2012, Claessens & Tilley 2014, Nelson *et al.* 2014). The goal of current treatments of CRPC is to maximally suppress androgen signaling, which may in turn remove the androgen suppression of GPR30 expression, resulting in a high level of GPR30 in late-stage CRPC. In this study, we provided convincing evidence that, in both a preclinical model and in human specimens, reduced androgen levels in CRPC enhanced GPR30 expression when compared with hormone-naïve PC. The wide expression and high levels of GPR30 may highlight an unprecedented opportunity to target this protein in clinical metastases of CRPC.

Existing therapies for CRPC offer limited gains in survival and trigger adverse effects; thus, attention has begun to focus on the sequence of application of these treatments (Higano & Crawford 2011). The current LNCaP model represents a subtype of CRPC in which G-1 induced intra-tumoral neutrophil infiltration associated with

tumor necrosis. Similarly, we reasoned that a subset of patients harboring CRPC may benefit from G-1 therapy if it is delivered before the patients receive chemotherapy, which can compromise neutrophil production. In light of the most recent CRPC that failed second-generation ADT (i.e. abiraterone acetate and MDV3100), whether or not the expression of GPR30 or the population of patients expressing high levels of GPR30 is increased upon resistance is a clinically interesting question with respect to the further exploration of GPR30 as a novel targeted therapy for late-stage CRPC. Importantly, in all the animal studies reported to date, G-1 did not induce adverse effects (Blasko *et al.* 2009, Dennis *et al.* 2009, Chan *et al.* 2010, Gao *et al.* 2011). G-1 toxicity to the functions of vital organs including heart and liver has been further proven to be undetectable in this study. One major concern regarding estrogen-related treatment in PC is the increase in the risk of venous thromboembolism (reviewed in Cox & Crawford (1995)). Although G-1 is a specific GPR30 agonist that has been shown not to bind ER $\alpha$  at a concentration up to 10  $\mu$ M (Bologa *et al.* 2006), definitive evidence for the absence of estrogen-mediated coagulation *in vivo* is required.

Our findings, taken together, indicated that G-1 effectively inhibited preclinical CRPC growth with a low risk of toxicity; underscoring that G-1 or other GPR30-specific agonists might serve as novel anticancer agents for CRPC that expresses GPR30. The upregulation of GPR30 expression after androgen ablation and the recruitment of neutrophils to the CR tumors are both indicative of a potentially important therapeutic window for G-1/GPR30-targeted therapy preferably under the conditions of a low or ultra-low androgen levels in CRPC before chemotherapy.

#### Supplementary data

This is linked to the online version of the paper at <http://dx.doi.org/10.1530/ERC-14-0402>.

#### Declaration of interest

The authors declare that there is no conflict of interest that could be perceived as prejudicing the impartiality of the research reported.

#### Funding

This work was supported by Veteran Affairs (Merit Award I01BX000675 to S-M Ho), the National Institutes of Health (grant numbers P30E5006096, U01ES019480, and U01ES020988 to S-M Ho and P50CA097186 Pacific Northwest SPORE Career Development Award to H-M Lam), and the Prostate Cancer Foundation (Young Investigator Award to H-M Lam).

### Acknowledgements

The authors thank the Genomics, Epigenomics and Sequencing Core at the University of Cincinnati for Affymetrix microarray experiments, Ms Dan Song for her support during the immunohistochemistry study, Dr Yuet-Kin Leung for critical reading of the manuscript, and Ms Nancy K Voynow for her professional editing of this manuscript.

### References

- Ahola TM, Purmonen S, Pennanen P, Zhuang YH, Tuohimaa P & Ylikomi T 2002 Progesterone upregulates G-protein-coupled receptor 30 in breast cancer cells. *European Journal of Biochemistry* **269** 2485–2490. (doi:10.1046/j.1432-1033.2002.02912.x)
- Albanito L, Madeo A, Lappano R, Vivacqua A, Rago V, Carpino A, Oprea TI, Prossnitz ER, Musti AM, Ando S et al. 2007 G protein-coupled receptor 30 (GPR30) mediates gene expression changes and growth response to 17 $\beta$ -estradiol and selective GPR30 ligand G-1 in ovarian cancer cells. *Cancer Research* **67** 1859–1866. (doi:10.1158/0008-5472.CAN-06-2909)
- Albanito L, Sisci D, Aquila S, Brunelli E, Vivacqua A, Madeo A, Lappano R, Pandey DP, Picard D, Mauro L et al. 2008 Epidermal growth factor induces G protein-coupled receptor 30 expression in estrogen receptor-negative breast cancer cells. *Endocrinology* **149** 3799–3808. (doi:10.1210/en.2008-0117)
- Blasko E, Haskell CA, Leung S, Gualtieri G, Halks-Miller M, Mahmoudi M, Dennis MK, Prossnitz ER, Karpus WJ & Horuk R 2009 Beneficial role of the GPR30 agonist G-1 in an animal model of multiple sclerosis. *Journal of Neuroimmunology* **214** 67–77. (doi:10.1016/j.jneuroim.2009.06.023)
- Bologa CG, Revankar CM, Young SM, Edwards BS, Arterburn JB, Kiselyov AS, Parker MA, Tkachenko SE, Savchuck NP, Sklar LA et al. 2006 Virtual and biomolecular screening converge on a selective agonist for GPR30. *Nature Chemical Biology* **2** 207–212. (doi:10.1038/nchembio775)
- de Bono JS, Oudard S, Ozguroglu M, Hansen S, Machiels JP, Kocak I, Gravis G, Bodrogi I, Mackenzie MJ, Shen L et al. 2010 Prednisone plus cabazitaxel or mitoxantrone for metastatic castration-resistant prostate cancer progressing after docetaxel treatment: a randomised open-label trial. *Lancet* **376** 1147–1154. (doi:10.1016/S0140-6736(10)61389-X)
- de Bono JS, Logothetis CJ, Molina A, Fizazi K, North S, Chu L, Chi KN, Jones RJ, Goodman OB Jr, Saad F et al. 2011 Abiraterone and increased survival in metastatic prostate cancer. *New England Journal of Medicine* **364** 1995–2005. (doi:10.1056/NEJMoa1014618)
- Cacalano G, Lee J, Kikly K, Ryan AM, Pitts-Meek S, Hultgren B, Wood WI & Moore MW 1994 Neutrophil and B cell expansion in mice that lack the murine IL-8 receptor homolog. *Science* **265** 682–684. (doi:10.1126/science.8036519)
- Caruso RA, Bellocco R, Pagano M, Bertoli G, Rigoli L & Inferrera C 2002 Prognostic value of intratumoral neutrophils in advanced gastric carcinoma in a high-risk area in northern Italy. *Modern Pathology* **15** 831–837. (doi:10.1097/01.MP.0000020391.98998.6B)
- Chan QK, Lam HM, Ng CF, Lee AY, Chan ES, Ng HK, Ho SM & Lau KM 2010 Activation of GPR30 inhibits the growth of prostate cancer cells through sustained activation of Erk1/2, c-jun/c-fos-dependent upregulation of p21, and induction of G<sub>2</sub> cell-cycle arrest. *Cell Death and Differentiation* **17** 1511–1523. (doi:10.1038/cdd.2010.20)
- Cheng SB, Graeber CT, Quinn JA & Filardo EJ 2011 Retrograde transport of the transmembrane estrogen receptor, G-protein-coupled-receptor-30 (GPR30/GPER) from the plasma membrane towards the nucleus. *Steroids* **76** 892–896. (doi:10.1016/j.steroids.2011.02.018)
- Claessens F & Tilley W 2014 Androgen signaling and steroid receptor crosstalk in endocrine cancers. *Endocrine-Related Cancer* **21** E3–E5. (doi:10.1530/ERC-14-0274)
- Cox RL & Crawford ED 1995 Estrogens in the treatment of prostate cancer. *Journal of Urology* **154** 1991–1998. (doi:10.1016/S0022-5347(01)66670-9)
- Decker KF, Zheng D, He Y, Bowman T, Edwards JR & Jia L 2012 Persistent androgen receptor-mediated transcription in castration-resistant prostate cancer under androgen-deprived conditions. *Nucleic Acids Research* **40** 10765–10779. (doi:10.1093/nar/gks888)
- De Marco P, Bartella V, Vivacqua A, Lappano R, Santolla MF, Morcavallo A, Pezzi V, Belfiore A & Maggiolini M 2013 Insulin-like growth factor-I regulates GPER expression and function in cancer cells. *Oncogene* **32** 678–688. (doi:10.1038/onc.2012.97)
- Dennis MK, Burai R, Ramesh C, Petrie WK, Alcon SN, Nayak TK, Bologa CG, Leitao A, Brailoiu E, Deliu E et al. 2009 *In vivo* effects of a GPR30 antagonist. *Nature Chemical Biology* **5** 421–427. (doi:10.1038/nchembio.168)
- Di Carlo E, Forni G, Lollini P, Colombo MP, Modesti A & Musiani P 2001 The intriguing role of polymorphonuclear neutrophils in antitumor reactions. *Blood* **97** 339–345. (doi:10.1182/blood.V97.2.339)
- Eash KJ, Greenbaum AM, Gopalan PK & Link DC 2010 CXCR2 and CXCR4 antagonistically regulate neutrophil trafficking from murine bone marrow. *Journal of Clinical Investigation* **120** 2423–2431. (doi:10.1172/JCI41649)
- Filardo EJ, Quinn JA, Bland KI & Frackelton AR Jr 2000 Estrogen-induced activation of Erk-1 and Erk-2 requires the G protein-coupled receptor homolog, GPR30, and occurs via *trans*-activation of the epidermal growth factor receptor through release of HB-EGF. *Molecular Endocrinology* **14** 1649–1660. (doi:10.1210/mend.14.10.0532)
- Fu X, Tao L, Rivera A, Xu H & Zhang X 2011 Virotherapy induces massive infiltration of neutrophils in a subset of tumors defined by a strong endogenous interferon response activity. *Cancer Gene Therapy* **18** 785–794. (doi:10.1038/cgt.2011.46)
- Funakoshi T, Yanai A, Shinoda K, Kawano MM & Mizukami Y 2006 G protein-coupled receptor 30 is an estrogen receptor in the plasma membrane. *Biochemical and Biophysical Research Communications* **346** 904–910. (doi:10.1016/j.bbrc.2006.05.191)
- Gao F, Ma X, Ostmann AB & Das SK 2011 GPR30 activation opposes estrogen-dependent uterine growth via inhibition of stromal ERK1/2 and estrogen receptor alpha (ER $\alpha$ ) phosphorylation signals. *Endocrinology* **152** 1434–1447. (doi:10.1210/en.2010-1368)
- Geiser T, Dewald B, Ehrenguber MU, Clark-Lewis I & Baggiolini M 1993 The interleukin-8-related chemotactic cytokines GRO $\alpha$ , GRO $\beta$ , and GRO $\gamma$  activate human neutrophil and basophil leukocytes. *Journal of Biological Chemistry* **268** 15419–15424.
- Gregory AD & Houghton AM 2011 Tumor-associated neutrophils: new targets for cancer therapy. *Cancer Research* **71** 2411–2416. (doi:10.1158/0008-5472.CAN-10-2583)
- Haas E, Meyer MR, Schurr U, Bhattacharya I, Minotti R, Nguyen HH, Heigl A, Lachat M, Genoni M & Barton M 2007 Differential effects of 17 $\beta$ -estradiol on function and expression of estrogen receptor  $\alpha$ , estrogen receptor  $\beta$ , and GPR30 in arteries and veins of patients with atherosclerosis. *Hypertension* **49** 1358–1363. (doi:10.1161/HYPERTENSIONAHA.107.089995)
- Harokopakis E & Hajishengallis G 2005 Integrin activation by bacterial fimbriae through a pathway involving CD14, Toll-like receptor 2, and phosphatidylinositol-3-kinase. *European Journal of Immunology* **35** 1201–1210. (doi:10.1002/eji.200425883)
- Higano CS & Crawford ED 2011 New and emerging agents for the treatment of castration-resistant prostate cancer. *Urologic Oncology* **29** S1–S8. (doi:10.1016/j.urolonc.2011.08.013)
- Higano CS, Schellhammer PF, Small EJ, Burch PA, Nemunaitis J, Yuh L, Provost N & Frohlich MW 2009 Integrated data from 2 randomized, double-blind, placebo-controlled, phase 3 trials of active cellular immunotherapy with sipuleucel-T in advanced prostate cancer. *Cancer* **115** 3670–3679. (doi:10.1002/cncr.24429)
- Hirose K, Hakozaki M, Nyunoya Y, Kobayashi Y, Matsushita K, Takenouchi T, Mikata A, Mukaida N & Matsushima K 1995 Chemokine gene transfection into tumour cells reduced tumorigenicity in nude mice in association with neutrophilic infiltration. *British Journal of Cancer* **72** 708–714. (doi:10.1038/bjc.1995.398)

- Ho SM, Lee MT, Lam HM & Leung YK 2011 Estrogens and prostate cancer: etiology, mediators, prevention, and management. *Endocrinology and Metabolism Clinics of North America* **40** 591–614. (doi:10.1016/j.ecl.2011.05.002)
- Huang HJ, Neven P, Drijkoningen M, Paridaens R, Wildiers H, Van Limbergen E, Berteloot P, Amant F, Vergote I & Christiaens MR 2005 Association between tumour characteristics and HER-2/neu by immunohistochemistry in 1362 women with primary operable breast cancer. *Journal of Clinical Pathology* **58** 611–616. (doi:10.1136/jcp.2004.022772)
- Huggins C & Hodges CV 2002 Studies on prostatic cancer: I. The effect of castration, of estrogen and of androgen injection on serum phosphatases in metastatic carcinoma of the prostate. 1941. *Journal of Urology* **168** 9–12. (doi:10.1016/S0022-5347(05)64820-3)
- Jacobi JS, Martin C, Nava G, Jeziorski MC, Clapp C & Martinez de la EG 2007 17- $\beta$ -estradiol directly regulates the expression of adrenergic receptors and kisspeptin/GPR54 system in GT1-7 GnRH neurons. *Neuroendocrinology* **86** 260–269. (doi:10.1159/000107770)
- Kantoff PW, Higano CS, Shore ND, Berger ER, Small EJ, Penson DF, Redfern CH, Ferrari AC, Dreicer R, Sims RB *et al.* 2010 Sipuleucel-T immunotherapy for castration-resistant prostate cancer. *New England Journal of Medicine* **363** 411–422. (doi:10.1056/NEJMoa1001294)
- Langley RE, Cafferty FH, Alhasso AA, Rosen SD, Sundaram SK, Freeman SC, Pollock P, Jinks RC, Godsland IF, Kockelbergh R *et al.* 2013 Cardiovascular outcomes in patients with locally advanced and metastatic prostate cancer treated with luteinising-hormone-releasing-hormone agonists or transdermal oestrogen: the randomised, phase 2 MRC PATCH trial (PR09). *Lancet Oncology* **14** 306–316. (doi:10.1016/S1470-2045(13)70025-1)
- Leav I, Lau KM, Adams JY, McNeal JE, Taplin ME, Wang J, Singh H & Ho SM 2001 Comparative studies of the estrogen receptors  $\beta$  and  $\alpha$  and the androgen receptor in normal human prostate glands, dysplasia, and in primary and metastatic carcinoma. *American Journal of Pathology* **159** 79–92. (doi:10.1016/S0002-9440(10)61676-8)
- Leung BP, Culshaw S, Gracie JA, Hunter D, Canetti CA, Campbell C, Cunha F, Liew FY & McInnes IB 2001 A role for IL-18 in neutrophil activation. *Journal of Immunology* **167** 2879–2886. (doi:10.4049/jimmunol.167.5.2879)
- Leung YK, Lam HM, Wu S, Song D, Levin L, Cheng L, Wu CL & Ho SM 2010 Estrogen receptor  $\beta$ 2 and  $\beta$ 5 are associated with poor prognosis in prostate cancer, and promote cancer cell migration and invasion. *Endocrine-Related Cancer* **17** 675–689. (doi:10.1677/ERC-09-0294)
- Madeo A & Maggiolini M 2010 Nuclear alternate estrogen receptor GPR30 mediates 17 $\beta$ -estradiol-induced gene expression and migration in breast cancer-associated fibroblasts. *Cancer Research* **70** 6036–6046. (doi:10.1158/0008-5472.CAN-10-0408)
- Maggiolini M & Picard D 2010 The unfolding stories of GPR30, a new membrane-bound estrogen receptor. *Journal of Endocrinology* **204** 105–114. (doi:10.1677/JOE-09-0242)
- Musiani P, Allione A, Modica A, Lollini PL, Giovarelli M, Cavallo F, Belardelli F, Forni G & Modesti A 1996 Role of neutrophils and lymphocytes in inhibition of a mouse mammary adenocarcinoma engineered to release IL-2, IL-4, IL-7, IL-10, IFN- $\alpha$ , IFN- $\gamma$ , and TNF- $\alpha$ . *Laboratory Investigation* **74** 146–157.
- Nelson AW, Tilley WD, Neal DE & Carroll JS 2014 Estrogen receptor beta in prostate cancer: friend or foe? *Endocrine-Related Cancer* **21** T219–T234. (doi:10.1530/ERC-13-0508)
- Norman G, Dean ME, Langley RE, Hodges ZC, Ritchie G, Parmar MK, Sydes MR, Abel P & Eastwood AJ 2008 Parenteral oestrogen in the treatment of prostate cancer: a systematic review. *British Journal of Cancer* **98** 697–707. (doi:10.1038/sj.bjc.6604230)
- Oh WK 2002 The evolving role of estrogen therapy in prostate cancer. *Clinical Prostate Cancer* **1** 81–89. (doi:10.3816/CGC.2002.n.009)
- Otto C, Rohde-Schulz B, Schwarz G, Fuchs I, Klewer M, Brittain D, Langer G, Bader B, Prella K, Nubbemeyer R *et al.* 2008 G protein-coupled receptor 30 localizes to the endoplasmic reticulum and is not activated by estradiol. *Endocrinology* **149** 4846–4856. (doi:10.1210/en.2008-0269)
- Pandey DP, Lappano R, Albanito L, Madeo A, Maggiolini M & Picard D 2009 Estrogenic GPR30 signalling induces proliferation and migration of breast cancer cells through CTGF. *EMBO Journal* **28** 523–532. (doi:10.1038/emboj.2008.304)
- Pelleitier M & Montplaisir S 1975 The nude mouse: a model of deficient T-cell function. *Methods and Achievements in Experimental Pathology* **7** 149–166.
- Prossnitz ER & Barton M 2011 The G-protein-coupled estrogen receptor GPER in health and disease. *Nature Reviews. Endocrinology* **7** 715–726. (doi:10.1038/nrendo.2011.122)
- Prossnitz ER, Arterburn JB & Sklar LA 2007 GPR30: a G protein-coupled receptor for estrogen. *Molecular and Cellular Endocrinology* **265** 138–142. (doi:10.1016/j.mce.2006.12.010)
- Recchia AG, De Francesco EM, Vivacqua A, Sisci D, Panno ML, Ando S & Maggiolini M 2011 The G protein-coupled receptor 30 is up-regulated by hypoxia-inducible factor-1 $\alpha$  (HIF-1 $\alpha$ ) in breast cancer cells and cardiomyocytes. *Journal of Biological Chemistry* **286** 10773–10782. (doi:10.1074/jbc.M110.172247)
- Ryckman C, Vandal K, Rouleau P, Talbot M & Tessier PA 2003 Proinflammatory activities of S100 proteins S100A8, S100A9, and S100A8/A9 induce neutrophil chemotaxis and adhesion. *Journal of Immunology* **170** 3233–3242. (doi:10.4049/jimmunol.170.6.3233)
- Saenko EL, Skorobogat'ko OV, Tarasenko P, Romashko V, Zhuravetz L, Zadorozhnaya L, Senjuk OF & Yaropolov AI 1994 Modulatory effects of ceruloplasmin on lymphocytes, neutrophils and monocytes of patients with altered immune status. *Immunological Investigations* **23** 99–114. (doi:10.3109/0882013940908792)
- Schaider H, Oka M, Bogenrieder T, Nesbit M, Satyamoorthy K, Berking C, Matsushima K & Herlyn M 2003 Differential response of primary and metastatic melanomas to neutrophils attracted by IL-8. *International Journal of Cancer* **103** 335–343. (doi:10.1002/ijc.10775)
- Schellhammer P 2012 Life after failure of traditional androgen deprivation therapy. *Urologic Oncology* **30** S10–S14. (doi:10.1016/j.urolonc.2012.01.009)
- Tannock IF, de Wit R, Berry WR, Horti J, Pluzanska A, Chi KN, Oudard S, Theodore C, James ND, Turesson I *et al.* 2004 Docetaxel plus prednisone or mitoxantrone plus prednisone for advanced prostate cancer. *New England Journal of Medicine* **351** 1502–1512. (doi:10.1056/NEJMoa040720)
- Thomas P, Pang Y, Filardo EJ & Dong J 2005 Identity of an estrogen membrane receptor coupled to a G protein in human breast cancer cells. *Endocrinology* **146** 624–632. (doi:10.1210/en.2004-1064)
- Vivacqua A, Bonofiglio D, Recchia AG, Musti AM, Picard D, Ando S & Maggiolini M 2006 The G protein-coupled receptor GPR30 mediates the proliferative effects induced by 17 $\beta$ -estradiol and hydroxytamoxifen in endometrial cancer cells. *Molecular Endocrinology* **20** 631–646. (doi:10.1210/me.2005-0280)
- Yang L, Ravindranathan P, Ramanan M, Kapur P, Hammes SR, Hsieh JT & Raj GV 2012 Central role for PELP1 in nonandrogenic activation of the androgen receptor in prostate cancer. *Molecular Endocrinology* **26** 550–561. (doi:10.1210/me.2011-1101)
- Zheng D, Decker KF, Zhou T, Chen J, Qi Z, Jacobs K, Weillbaeher KN, Corey E, Long F & Jia L 2013 Role of WNT7B-induced noncanonical pathway in advanced prostate cancer. *Molecular Cancer Research* **11** 482–493. (doi:10.1158/1541-7786.MCR-12-0520)

Received in final form 30 September 2014

Accepted 6 October 2014

Made available online as an Accepted Preprint

6 October 2014

## **Supplementary Methods**

### **Microarray experiment and analysis**

Microarrays were performed as previously described (1). In brief, 15 µg of fragmented amplified RNA was hybridized to Human Gene 1.0 ST Array, stained, and washed according to the manufacturer's protocols (Affymetrix, Santa Clara, CA). The signals were scanned with Affymetrix GeneChip Scanner 3000 7G with GCOS software. The microarray data were analyzed with statistical software R and the limma package of Bioconductor (2) with custom CDF downloaded from BrainArray (3). Data preprocessing, including background correction and normalization, was performed with Robust Multi-array Average (RMA). Array quality was assessed with the Quality Metrics package of Bioconductor (4). Differentially expressed genes were identified by comparing four treatments based on data from four independent biological replicates per group by one-way ANOVA. Hierarchical gene and sample clustering was computed using Euclidean distance and agglomerating nodes by average linkage. Castrated G-1-specific genes (vs. castrated vehicle genes) were identified by two-group comparison with limma, and resulting t-statistics were modified by an intensity-based empirical Bayes method (IBMT) (5). Genes with  $p < 0.01$  were considered to be significantly differentially expressed (560 genes). Significantly altered genes with a fold change greater than 1.5 fold between castrated G-1 versus control group (99 genes) were imported to Ingenuity Pathway Analysis (IPA, Ingenuity Systems; <https://www.ingenuity.com>) to identify enriched biological pathways. IPA is a repository of biological interactions and functional annotations to demonstrate relationships among proteins, genes, complexes, metabolites, and drugs.

### **Histopathology and immunohistochemistry experiments**

Antibodies and staining conditions for GPR30, proliferation (Ki67), apoptosis (cleaved caspase-3), blood vessel (CD31), T cells (CD3), B cells (CD45R), neutrophils (NIMP-R14), and macrophages (F4/80) are presented in Table S2. Sections of mouse spleen, mouse prostate, and human prostate were included in staining procedures as positive controls, wherever appropriate, with the omission of primary antibody serving as the negative staining control. The specificity of GPR30 antibody was determined by neutralizing the antibody with a 10× excess by weight of the immunizing peptide (MBL International, Woburn, MA) overnight at 4 °C. The antibody-peptide precipitate was removed by centrifugation at 12,000 ×g for 10 min, and the supernatant (preabsorbed antibody) was used in the IHC study. All antibodies were incubated on slides overnight at 4 °C.

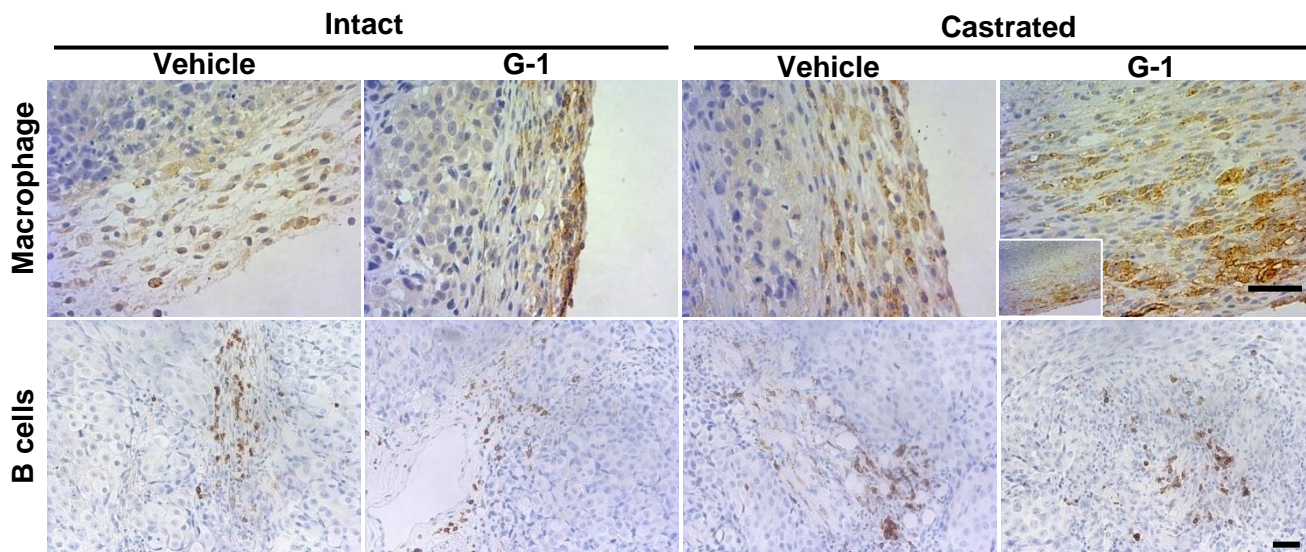
Digital images were collected with an AxioCam MRm camera mounted on an Axiovert 200M microscope and analyzed with Axiovision 4.7 software (Carl Zeiss, Thornwood, NY). Sections were scanned at ×40 or ×100 to localize representative areas for quantitation. For the analysis of necrosis, four ×40 fields were measured for an individual tumor to determine the percentage of necrosis (i.e., sum of necrotic area/total section area). For quantification of TUNEL and Ki67 staining, five representative ×200 fields (>1,000 cells/section, n=7 animals per group) were acquired using Axiovision 4.7 software (Carl Zeiss), and positively stained cells were counted using ImageJ software (Research Services Branch, National Institute of Mental Health, Bethesda, MD) and compared with the manual counting of the same sections by another investigator. Data for each treatment group are presented as the mean percentage of positive cells per total cells counted in six or seven animals. For CD31 staining of vasculature, three representative ×100 fields were acquired in the stroma and capsule. The mean vessel density (MVD) was calculated

as the average number of vessels per field ( $\mu\text{m}^2$ ), and the mean vessel area (MVA) was calculated as the average area of vessels per field ( $\mu\text{m}^2$ ).

## References

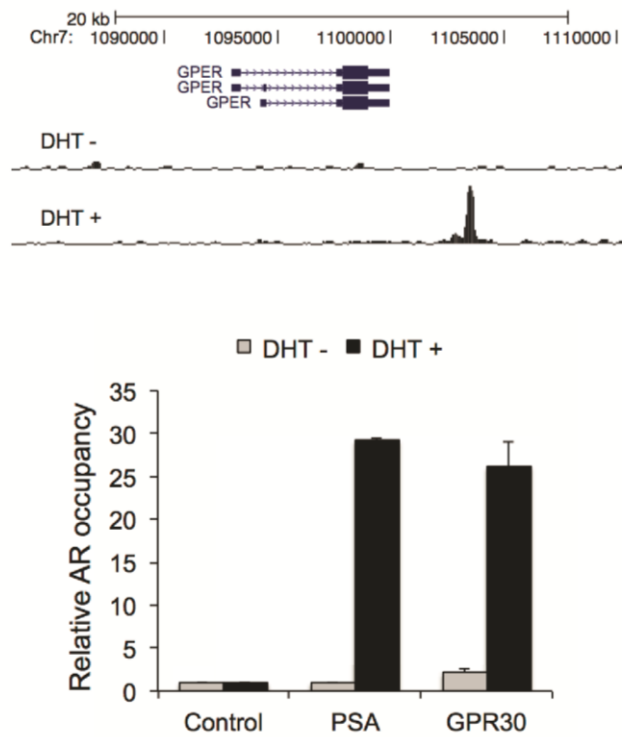
- (1) Tam NN, Szeto CY, Freudenberg JM, Fullenkamp AN, Medvedovic M, Ho SM. Research resource: estrogen-driven prolactin-mediated gene-expression networks in hormone-induced prostatic intraepithelial neoplasia. *Mol Endocrinol.* 2010;24(11):2207-2217.
- (2) Smyth GK. Linear models and empirical bayes methods for assessing differential expression in microarray experiments. *Stat. Appl. Genet. Mol. Biol.* 2004;3: Article3.
- (3) Dai M, Wang P, Boyd AD, Kostov G, Athey B, Jones EG, et al. Evolving gene/transcript definitions significantly alter the interpretation of GeneChip data. *Nucleic Acids Res.* 2005;33:e175.
- (4) Kauffmann A, Gentleman R, Huber W. arrayQualityMetrics—a bioconductor package for quality assessment of microarray data. *Bioinformatics.* 2009;25(3): 415–416.
- (5) Sartor MA, Leikauf GD, Medvedovic M. LRpath: a logistic regression approach for identifying enriched biological groups in gene expression data. *Bioinformatics.* 2009;25(2): 211–217.

Figure S1



IHC staining of macrophages and B cells in LNCaP xenografts. Macrophages were detected in the tumor capsule, and B cells were exclusively found in the intra-tumoral stroma in both vehicle and G-1 treated groups in intact or castrated host. Magnification: 200x (macrophage); 100x (macrophage insert and B cells). Scale bars represent 50 $\mu$ m in all micrographs.

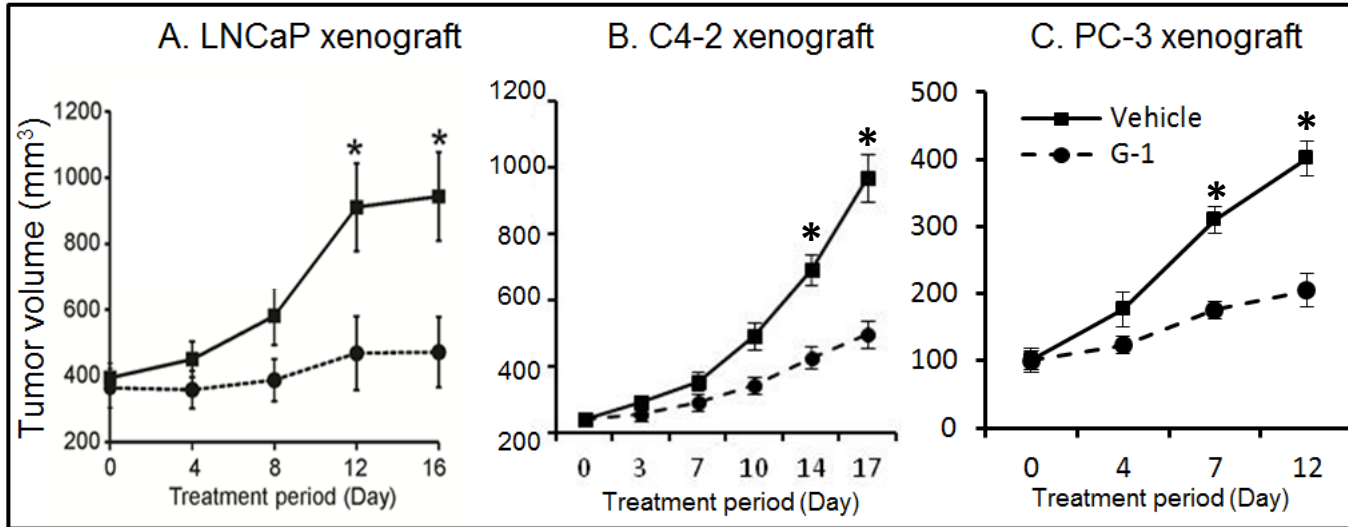
Figure S2



ChIP-seencing results showing AR binding to the GPER (GPR30) locus after 4h DHT treatment in LNCaP cells (upper panel) and ChIP-qPCR analyses were conducted to confirm the ChIP-seencing results (lower panel). The PSA enhancer was used as a positive control. AR occupancy at the negative control region was defined as 1. ChIP, chromatin immunoprecipitation.

Figure S3

Xenograft in castrated mice



G-1 inhibited castration-resistant tumor growth. A) G-1 inhibited LNCaP xenograft tumor growth in castrated mice but not in intact mice (data from the current manuscript). Xenografts were established from androgen-dependent cell line LNCaP. When tumors grew to 150-300 mm<sup>3</sup>, mice were divided into two groups: intact and castrated. For intact animals (Fig.1A), mice were injected subcutaneously with vehicle or G-1 (4mg/kg/day) for 16 days. For castrated animals (Fig.1B), mice were castrated and, when the tumor resumes growing, were treated with vehicle or G-1 for 16 days. G-1 inhibited growth of B) C4-2 xenografts (unpublished data) and C) PC-3 xenografts (Chan *et al* 2010 Cell Death Differ. 17:1511-23), all growing in castrated hosts. Nude mice were castrated and subcutaneously inoculated with castration-resistance prostate cancer cell lines C4-2 or PC-3. When tumor grew to 200 mm<sup>3</sup>, mice were divided into two groups and treated with vehicle and G-1 as the same dose as above for 17 days or 12 days, respectively.

**Table S1. Primer sequences used in real-time RT-PCR analysis**

	Gene	Forward	Reverse	Amplicon size (bp)	Entrez ID
<b>Human</b>	<i>ActB</i>	CGTCGACAACGGCTCCGGCATG	CCACCATCACACCCTGGTGCCTAGG	110	NM_001101
	<i>AR</i>	TGTCCATCTTGTCTGCTTCG	ATGGCTTCCAGGACATTCAG	209	NM_000044
	<i>CCL2</i>	CTGAAGCTCGCACTCTCGCCT	GGCATTGATTGCATCTGGCTGAGC	116	NM_002982
	<i>CP</i>	CGGTCTGGCTTGGGTTTTTAGGCC	AGGGTAGATGGCCCCCTCATGT	149	NM_000096
	<i>CXCL12</i>	CGATTCTTCGAAAGCCATGT	CTTTAGCTTCGGGTCAATGC	135	NM_199168
	<i>GAPDH</i>	TCCCTGAGCTGAACGGGAAG	GGAGGAGTGGGTGTCTGCTGT	198	NM_002046
	<i>GPR30</i>	GCGGGTCTCTTCTCTCTCT	CGTGGAGCTGCTCACTCTCT	172	NM_001098201
	<i>IFI44</i>	ACGCTGGTGTGGTACATGTGGC	CCTCTAGCTTGGACCTCACAGGCT	114	NM_006417
	<i>IFIT2</i>	TGCACTGCAACCATGAGTGAGAACA	GCCAGTAGGTTGCACATTGTGGC	185	NM_001547
	<i>IFIT3</i>	TGGGCCGCCTGCTAAGGGAT	ACTGCGCCCTGGCCCATTTC	100	NM_001549
	<i>IL8</i>	AAAAGCCACCGGAGCACTCCA	ACTGCACCTTCACACAGAGCTGCA	188	NM_000584
	<i>PSA</i>	AGCATTGAAC-CAGAGGAGTTCT	CCCAGCAGGCTGCTTTTG	157	NM_001030048
<i>SOD2</i>	ACAGGCCTTATTCCACTGCT	CAGCATAACGATCGTGGTTT	168	NM_000636	
<b>Mouse</b>	<i>Cd14</i>	GGCCGCGCGGATTCCTAGTC	ATCGGGTCCGGTGGCTTCCA	139	NM_009841
	<i>Cxcl1</i>	TGATCCCAGCCACCCGCTCG	ACAGCGCAGCTCATTGGCGAT	98	NM_008176
	<i>Cxcl12</i>	GCTCTGCATCAGTGACGGTA	TAATTCGGGTCAATGCACA	184	NM_001012477
	<i>Cxcl3</i>	CTTGACGGTGACGCCCCCAG	CCCGGCTCAGCTGGACTTGC	154	NM_203320
	<i>Il18</i>	GGCCGACTTCACTGTACAACCGC	TGGTCTGGGGTTCCTGACT	127	NM_008360
	<i>Il1b</i>	TCCTTGTGCAAGTGTCTGAAGCAGC	GGACAGCCCAGGTCAAAGGTTTGG	154	NM_008361
	<i>Il6</i>	TCTCTGCAAGAGACTTCCATCCAGT	TCCTCTGTGAAGTCTCCTCTCCGG	103	NM_031168
	<i>S100a8</i>	TCGAGGAGTTCCTTGCGATGGTG	GGACCCAGCCCTAGGCCAGAA	95	NM_013650
	<i>S100a9</i>	GGACACCCTGACACCCTGAGCA	CCTGGTTTGTGTCCAGGTCCTCCA	133	NM_009114
	<i>Tnf<math>\alpha</math></i>	TGCCCCGACTACGTGCTCCT	CCTTGGGGCAGGGGCTCTTG	103	NM_013693

Note: Forward and reverse primers were designed to recognize different exons of the target gene, except *Cd14* and *S100a8*.

**Table S2. Antibodies and staining conditions for immunohistochemistry study**

<b>Antibody</b>	<b>Dilution</b>	<b>Secondary antibody</b>	<b>Antigen retrieval</b>	<b>Source*</b>
<b>GPR30</b>	1:200	Anti-rabbit	Sodium citrate	MBL International
<b>Ki67</b>	1:100	Anti-mouse	Sodium citrate	Novocastra
<b>Cleaved Caspase-3</b>	1:100	Anti-rabbit	Sodium citrate	Cell Signaling
<b>CD31</b>	1:100	Anti-rabbit	Sodium citrate	Abcam
<b>CD3</b>	1:100	Anti-rabbit	Sodium citrate	Abcam
<b>CD45R</b>	1:50	Anti-rat	No	Abcam
<b>NIMP-R14</b>	1:100	Anti-rat	No	Abcam
<b>F4/80</b>	1:100	Anti-rat	Sodium citrate	Abcam

The primary antibodies were diluted in 10% normal horse serum (for Ki67) or normal goat serum (all the others) in PBS in accordance with the recommended concentrations. \*MBL International: Woburn, MA ; Abcam: Cambridge, MA; Novocastra: Newcastle upon Tyne, UK

**Table S3. Top canonical pathways and biological networks represented by the G-1-induced differentially expressed genes in castration-resistant LNCaP xenografts using Ingenuity Pathway Analysis.**

<b>Top canonical pathways</b>	
<b>Name</b>	<b><i>p</i> value</b>
Communication between innate and adaptive immune cells	3.34E-03
Antigen presentation pathway	7.65E-03
P2Y purigenic receptor signaling pathway	8.61E-03
Melatonin signaling	2.53E-02
Caveolar-mediated endocytosis signaling	2.59E-02
<b>Top biological networks</b>	
<b>Name</b>	<b><i>p</i> value</b>
Antigen presentation, cell-to-cell signaling and interaction, inflammatory response	1E-29
Genetic disorder, neurological disease, skeletal and muscular disorders	1E-36
Carbohydrate metabolism, small molecule biochemistry, cell cycle	1E-22
Cell death, cellular assembly and organization, cellular function and maintenance	1E-21
Cell-to-cell signaling and interaction, cellular assembly and organization, nervous system development and function	1E-02

**Table S4. Summary of patient characteristics and baseline information for Cohorts 1 and 2**

Characteristics	Category	Descriptive Statistics			p <sup>c</sup>
		H-score = 0	H-score < 100	H-score ≥ 100	
<b>Primary PCa</b>		<b>N=5</b>	<b>N=103</b>	<b>N=124</b>	
Age (year) <sup>a</sup>		62 ± 8	62 ± 6	62 ± 7	0.732
Race/Ethnicity <sup>b</sup>	Asian	0 (0%)	2 (2%)	1 (1%)	0.848
	Black	0 (0%)	5 (5%)	4 (3%)	
	Hispanic	0 (0%)	1 (1%)	4 (3%)	
	White	5 (100%)	95 (92%)	115 (93%)	
Membrane staining <sup>b</sup>	Yes	0 (0%)	20 (19%)	56 (45%)	<.0001
Gleason Score <sup>b</sup>	<7	1 (20%)	40 (39%)	53 (43%)	0.687
	=7	3 (60%)	50 (49%)	51 (41%)	
	>7	1 (20%)	13 (13%)	20 (16%)	
Pre-operative serum PSA (ng/mL) <sup>a</sup>		2.0 ± 3.2	7.8 ± 5.4	8.6 ± 6.4	0.130
<b>Metastatic CRPC</b>		<b>N=0</b>	<b>N=6</b>	<b>N=18</b>	
Age (year) <sup>a</sup>			67 ± 10	62 ± 8	0.288
Gleason Score <sup>b</sup>	<7		0 (0.0%)	2 (11.1%)	0.721
	=7		1 (16.7%)	4 (22.2%)	
	>7		3 (50.0%)	9 (50.0%)	
	Missing		2 (33.3%)	3 (16.7%)	
Final Serum PSA (ng/mL) <sup>a</sup>			866.7 ± 876.0	709.8 ± 766.8	0.698
ADT Duration (years) <sup>a</sup>			5 ± 4	4 ± 2	0.640
ADT Type <sup>b</sup>	Lupron + Bicalutamide		2 (33.3%)	11 (61.1%)	0.481
	Lupron + Flutamide		2 (33.3%)	3 (16.6%)	
	Others		2 (33.3%)	4 (22.2%)	

a: Numerical variables are summarized by mean  $\pm$  std.

b: Categorical variables are summarized by frequency (in %).

c: p-values are from one way ANOVA tests and t-tests for numerical variables in Cohorts 1 and 2; and Chi-square tests for categorical variables, respectively.

**Table S5. GPR30 H-score among different bone locations of castration-resistant prostate cancer metastases in clinical specimens**

Variance	Pelvis/Sternum/Ischium/Iliac/Sacrum (n=16)		Rib/Limb (n= 15)		Spine (n=54)	
	H-score	S.E.	H-score	S.E.	H-score	S.E.
<b>H-score</b>	162.5	16.9	161.8	28.1	165.4	11.4
<b>Intensity</b>	1.6	0.2	1.6	0.3	1.7	0.1
<b>Stain %</b>	91.7	5.7	96.5	9.6	95.6	3.8

S.E.: stand error; n= number of metastases